SPHERICAL ZONE T-DESIGNS FOR NUMERICAL INTEGRATION AND APPROXIMATION *

CHAO LI† AND XIAOJUN CHEN‡

Abstract. In this paper, we present spherical zone t-designs, which provide quadrature rules with equal weight for spherical polynomials of degree at most t on a spherical zone $\{\mathbf{x} \in \mathbb{S}^2 : \cos\bar{\theta} \leq \mathbf{x}\cdot\mathbf{z} \leq \cos\underline{\theta}\}$ with $\mathbf{z} \in \mathbb{S}^2$ and $0 \leq \underline{\theta} < \bar{\theta} \leq \pi$. The spherical zone t-design is constructed by combining spherical t-designs and trapezoidal rules on $[0, 2\pi]$ with polynomial exactness t. We show that the spherical zone t-designs using spherical t-designs only provide quadrature rules with equal weight for spherical zonal polynomials of degree at most t on the spherical zone. We apply the proposed spherical zone t-designs to numerical integration, hyperinterpolation and sparse approximation on the spherical zone. Theoretical approximation error bounds are presented. Some numerical examples are given to illustrate the theoretical results and show the efficiency of the proposed spherical zone t-designs.

Key words. spherical designs, spherical zones, sparse optimization, trapezoidal rule

AMS subject classifications. 90C26, 90C90, 65D32

1. Introduction. A spherical t-design, introduced by Delsarte, Goethals and Seidel [15], is a set of points $\{\mathbf{x}_1, \ldots, \mathbf{x}_n\}$ on the unit sphere $\mathbb{S}^2 := \{\mathbf{x} \in \mathbb{R}^3 : \|\mathbf{x}\| = 1\}$ such that the following quadrature rule

$$\int_{\mathbb{S}^2} P(\mathbf{x}) d\omega(\mathbf{x}) = \frac{4\pi}{n} \sum_{i=1}^{n} P(\mathbf{x}_i), \quad \forall P \in \mathbb{P}_t(\mathbb{S}^2)$$

holds, where $\|\cdot\|$ is the Euclidean norm, $d\omega(\mathbf{x})$ is the surface measure on $\mathbb{S}^2$ and $\mathbb{P}_t(\mathbb{S}^2)$ is the space of all spherical polynomials of degree at most t. Seymour and Zaslavsky [24] proved the existence of spherical t-designs for arbitrary t if the number of points n is sufficiently large. Spherical t-designs have been extensively studied (see [6] for an excellent survey). Compared with nonequal positive weight quadrature rules on the sphere, spherical t-designs have shown promising prospects in various research areas, such as numerical integration and approximation over the sphere [1, 2], Lasso hyperinterpolation approximation [3], needlet approximation [30], sparse signal recovery [12], noisy data fitting [20].

Nowadays, there is a growing interest in numerical integration and approximation on subsets of the sphere. For any $\mathbf{z} \in \mathbb{S}^2$ and $\Theta = (\underline{\theta}, \bar{\theta})^\top$ with $0 \leq \underline{\theta} < \bar{\theta} \leq \pi$, we define a spherical zone $\mathcal{Z}(\mathbf{z}; \Theta)$ centered at $\mathbf{z}$ by

$$\mathcal{Z}(\mathbf{z}; \Theta) := \{\mathbf{x} \in \mathbb{S}^2 : \cos\bar{\theta} \leq \mathbf{x} \cdot \mathbf{z} \leq \cos\underline{\theta}\}.$$

The surface area of $\mathcal{Z}(\mathbf{z}; \Theta)$ is $|\mathcal{Z}(\mathbf{z}; \Theta)| := \int_{\mathcal{Z}(\mathbf{z};\Theta)} d\omega(\mathbf{x}) = 2\pi(\cos\underline{\theta} - \cos\bar{\theta})$. In particular, if $\underline{\theta} = 0$ and $\bar{\theta} \neq \pi$, then $\mathcal{C}(\mathbf{z}; \bar{\theta}) := \mathcal{Z}(\mathbf{z}; \Theta)$ is a spherical cap with center

*July 29, 2025

†School of Mathematics and Statistics, Taiyuan Normal University, Taiyuan, China; CAS AMSS-PolyU Joint Laboratory of Applied Mathematics, The Hong Kong Polytechnic University, Hong Kong, China (lichao.li@polyu.edu.hk). The work of this author is partially supported by National Natural Science Foundation of China (12301404) and Fund Program for the Scientific Activities of Selected Returned Overseas Professionals in Shanxi Province (20250034).

‡Department of Applied Mathematics, The Hong Kong Polytechnic University, Hong Kong, China (xiaojun.chen@polyu.edu.hk). The work of this author is supported by Hong Kong Research Grant Council PolyU15300123 and CAS-Croucher Funding Scheme for AMSS-PolyU Joint Laboratory.

$\mathbf{z} \in \mathbb{S}^2$ and angular radius $0 < \bar{\theta} < \pi$. If $\underline{\theta} = 0$ and $\bar{\theta} = \pi$, then $\mathcal{Z}(\mathbf{z}; \Theta) = \mathbb{S}^2$. Mhaskar [22] showed the existence of positive weight rules on a spherical cap by judiciously selecting nodes from a given set of scattered points on the spherical cap. Then, the author investigated the condition so that the results can be generalized to more general compact subsets of the sphere in [21]. Dai and Wang [14] proved that under certain conditions a positive weight rule with polynomial exactness t exists with t^2 points. Hesse and Womersley [18] showed the construction of positive weight quadrature rules with polynomial exactness t on spherical caps. Numerical quadrature and hyperinterpolation on spherical triangles using positive weight quadrature rules which are nearly exact for polynomials of certain degree are studied in [27, 28]. In [19], we proposed spherical cap t-subdesigns induced from spherical t-designs which are exact for spherical zonal polynomials of degree at most t and a class of orthonormal functions defined by shifted Legendre polynomials of degree at most t on spherical caps. We showed that spherical cap t-subdesigns are efficient for numerical integration and approximation on spherical caps.

Likewise, equidistant points on $[0, 2\pi]$ provide an equal weight quadrature rule on $[0, 2\pi]$, known as the trapezoidal rule (see for example [4, 29]), which is exact for all trigonometric polynomials of certain degree. Specifically,

$$\int_0^{2\pi} Q(\varphi) d\varphi = \frac{2\pi}{t+1} \sum_{i=1}^{t+1} Q(\varphi_i), \quad \forall Q \in \mathbb{Q}_t([0, 2\pi]), \tag{1.1}$$

where $\{\varphi_1, \ldots, \varphi_{t+1}\}$ is a set of equidistant points on $[0, 2\pi]$ with step size $2\pi/(t+1)$, $\mathbb{Q}_t([0, 2\pi]) := \operatorname{span}\{\frac{1}{2}, \cos\varphi, \sin\varphi, \ldots, \cos(t\varphi), \sin(t\varphi)\}$ is the space of all trigonometric polynomials of degree at most t on $[0, 2\pi]$. It is known that trapezoidal rules show good properties in numerical analysis and approximation theory (see [4, 29] and references therein). Especially, they show exponential convergence for approximating periodic functions with some smooth properties [29].

To the best of our knowledge, positive equal weight quadrature rules with polynomial exactness for numerical integration on spherical zones with $0 < \underline{\theta} < \bar{\theta} < \pi$ have not been developed. In this paper, we utilize spherical t-designs and trapezoidal rules on $[0, 2\pi]$ to construct equal weight quadrature rules on spherical zones.

Analogous to the definition of a spherical t-design, we give the definition of a spherical zone t-design as follows.

DEFINITION 1.1. *We call a set of points $\mathcal{X}_n := \{\mathbf{x}_1, \ldots, \mathbf{x}_n\}$ on a spherical zone $\mathcal{Z}(\mathbf{z}; \Theta)$ a spherical zone t-design if it holds that*

$$\int_{\mathcal{Z}(\mathbf{z};\Theta)} P(\mathbf{x}) d\omega(\mathbf{x}) = \frac{2\pi(\cos\underline{\theta} - \cos\bar{\theta})}{n} \sum_{i=1}^{n} P(\mathbf{x}_i), \quad \forall P \in \mathbb{P}_t(\mathbb{S}^2).$$

By the rotational invariance of the unit sphere $\mathbb{S}^2$, we first show that it is sufficient to construct spherical zone t-designs on the spherical zone $\mathcal{Z}(\mathbf{e}_3; \Theta)$ with center $\mathbf{e}_3 = (0, 0, 1)^\top$. Then, we construct spherical zone t-designs on a spherical zone $\mathcal{Z}(\mathbf{e}_3; \Theta)$ by combing spherical t-designs and trapezoidal rules (1.1) on $[0, 2\pi]$, which provide equal weight quadrature rules for spherical polynomials of degree at most t on the spherical zone. The polynomial exactness of the spherical zone t-design comes from the exactness of both spherical t-designs and trapezoidal rules (1.1) on $[0, 2\pi]$ with precision t. We give an example of a spherical zone 2-design with 6 points constructed from a tight spherical 2-design with 4 points and trapezoidal rules (1.1) on $[0, 2\pi]$

with $t = 2$. We indicate that the spherical zone t-design constructed using spherical t-designs only provide equal weight quadrature rules for spherical zonal polynomials. We also show that any positive weight quadrature rules with polynomial exactness t on the unit sphere $\mathbb{S}^2$ can induce a positive weight quadrature rule on the spherical zone $\mathcal{Z}(\mathbf{e}_3; \Theta)$ that is exact for both spherical harmonics of degree $\leq t$ and a class of orthonormal functions which are derived from shifted Legendre polynomials of degree at most t. This also contributes to the numerical integration of product of spherical harmonics on spherical zones with low computational cost. The present work provides some heuristic research for equal weight quadrature rules with polynomial exactness on spherical zones.

The main contributions of this paper are summarized as follows.

- We construct spherical zone t-designs on a spherical zone $\mathcal{Z}(\mathbf{e}_3; \Theta)$ with polynomial exactness t by combing spherical t-designs and trapezoidal rules (1.1) on $[0, 2\pi]$ with polynomial exactness t. We also present spherical zone t-designs for spherical zonal polynomials based on spherical t-designs only.
- We present positive weight quadrature rules with polynomial exactness on a spherical zone $\mathcal{Z}(\mathbf{e}_3; \Theta)$ induced by quadrature rules on the sphere $\mathbb{S}^2$. We show that the induced quadrature rules are exact for spherical harmonics, product of spherical harmonics and a class of orthonormal functions defined by shifted Legendre polynomials.
- We apply the spherical zone t-designs and Slepian functions to numerical integration and hyperinterpolation approximation on spherical zones. We also apply a capped-l_1 regularized minimization problem for approximation from noisy data on a spherical zone. Approximation error bounds are presented.

The paper is organized as follows. In section 2, we give notations and preliminaries. In section 3, we present positive weight quadrature rules, spherical zone t-designs on spherical zones and provide numerical integration error bounds. In section 4, we study hyperinterpolation and sparse approximations on spherical zones. In section 5, we present numerical results. Finally, we conclude the paper in section 6.

2. Notation and Preliminaries.

In this section, we summarize some notations and preliminaries used in this paper.

2.1. Notation.

Let $\mathbb{N}_0 := \{0, 1, 2, \ldots\}$ denote the set of natural numbers including zero. For any $t \in \mathbb{N}_0$, we denote $d_t := (t+1)^2$. The rotation group is denoted by $\mathrm{SO}(3) := \{\mathbf{R} \in \mathbb{R}^{3\times 3} : \mathbf{R}^\top \mathbf{R} = \mathbf{I}, \det \mathbf{R} = 1\}$, where $\mathbf{I} \in \mathbb{R}^{3\times 3}$ is the identity matrix. We use $\lfloor \cdot \rfloor$ and $\lceil \cdot \rceil$ to denote the floor and ceiling functions, respectively. $[\phi]_{\mathrm{mod}2\pi}$ means that ϕ is mapped into $[0, 2\pi]$ by adding $2k\pi$ with k being an integer as required. We denote by $\mathbb{L}_2(\Gamma)$ the space of square-integrable functions on a non-empty connected subset $\Gamma \subseteq \mathbb{S}^2$ endowed with the inner product

$$\langle f, g\rangle_{\mathbb{L}_2(\Gamma)} = \textstyle\int_\Gamma f(\mathbf{y})g(\mathbf{y})d\omega(\mathbf{y}), \quad \forall f, g \in \mathbb{L}_2(\Gamma),$$

and the $\mathbb{L}_2$ norm $\|f\|_{\mathbb{L}_2(\Gamma)} = (\langle f, f\rangle_{\mathbb{L}_2(\Gamma)})^{1/2}$. Let $\mathbb{C}(\Gamma)$ denote the space of continuous functions on Γ, $\|f\|_{\mathbb{L}_\infty(\Gamma)} := \sup_{\mathbf{x}\in\Gamma} |f(\mathbf{x})|$ for $f \in \mathbb{C}(\Gamma)$, and $\mathbb{P}_t(\Gamma)$ be the space of polynomials of degree $\leq t$ on Γ. And P_ℓ denotes a Legendre polynomial of degree ℓ defined as $P_\ell(x) := \frac{1}{2^\ell \ell!}\frac{d^\ell}{dx^\ell}(x^2-1)^\ell$, $\forall x \in [-1, 1]$.

2.2. Spherical harmonics and Slepian functions.

The standard basis for real-valued spherical harmonics of degree $\ell \in \mathbb{N}_0$ is (see for example [5])

$$Y_{\ell,1}(\vartheta, \phi) = N_{\ell,0} P_\ell(\cos\vartheta),$$

$$Y_{\ell,2m}(\vartheta,\phi) = N_{\ell,m}P_{\ell,m}(\cos\vartheta)\cos m\phi,$$
$$Y_{\ell,2m+1}(\vartheta,\phi) = N_{\ell,m}P_{\ell,m}(\cos\vartheta)\sin m\phi,\ m=1,\ldots,\ell,\ \forall(\vartheta,\phi)\in[0,\pi]\times[0,2\pi],$$

where $N_{\ell,m} = \sqrt{\frac{2\ell+1}{2\pi}\frac{(\ell-m)!}{(\ell+m)!}}$, $N_{\ell,0} = \sqrt{\frac{2\ell+1}{4\pi}}$ and $P_{\ell,m}$ is an associated Legendre function, i.e., $P_{\ell,m}(x) = (-1)^m(1-x^2)^{\frac{m}{2}}P_\ell^{(m)}(x)$, $\forall x\in[-1,1]$, $m=1,\ldots,\ell$, where $P_\ell^{(m)}$ denotes the mth derivative of a Legendre polynomial P_ℓ of degree ℓ. For any $\ell\in\mathbb{N}_0$, $Y_{\ell,1}$ is called a zonal spherical harmonic. For convenience, we denote by $Y_{\ell,k}$ a real-valued spherical harmonic of degree $\ell\in\mathbb{N}_0$, order $k\in\{1,\ldots,2\ell+1\}$ and write $Y_{\ell,k}(\mathbf{x}) := Y_{\ell,k}(\vartheta,\phi)$ with $\mathbf{x} = (\sin\vartheta\cos\phi, \sin\vartheta\sin\phi, \cos\vartheta)^\top\in\mathbb{S}^2$.

It is well-known that $\mathbb{P}_t(\mathbb{S}^2) := \mathrm{span}\{Y_{0,1}, Y_{1,1},\ldots,Y_{t,2t+1}\}$ (see for example [5]). Due to the loss of orthogonality of spherical harmonics on subsets of the unit sphere, we adopt the spherical Slepian functions [25]. For any non-empty connected subset $\Gamma\subset\mathbb{S}^2$ of the sphere and $t\in\mathbb{N}_0$, let $\mathbf{D}\in\mathbb{R}^{d_t\times d_t}$ be a matrix with elements

$$(\mathbf{D})_{\ell^2+k,\ell'^2+k'} = \int_\Gamma Y_{\ell,k}(\mathbf{x})Y_{\ell',k'}(\mathbf{x})d\omega(\mathbf{x}), \tag{2.1}$$

$\ell,\ell' = 0,1,\ldots,t$, $k=1,2,\ldots,2\ell+1$, $k'=1,2,\ldots,2\ell'+1$. From [25], $\mathbf{D}$ is a positive definite matrix and its eigenvalues satisfy $\lambda_i\in(0,1)$, $i=1,\ldots,d_t$. For convenience, we order the eigenvalues λ_i such that $1>\lambda_1\geq\ldots\geq\lambda_{d_t}>0$ with corresponding eigenvectors $\mathbf{v}_1,\ldots,\mathbf{v}_{d_t}$ (We choose $\mathbf{v}_1,\ldots,\mathbf{v}_{d_t}$ to be orthonormal). The real-valued Slepian functions [25] are defined by

$$S_i(\mathbf{x}) = \sum_{\ell=0}^{t}\sum_{k=1}^{2\ell+1} v_{\ell,k}^i Y_{\ell,k}(\mathbf{x}),\ i=1,2,\ldots,d_t,\quad \forall\mathbf{x}\in\mathbb{S}^2, \tag{2.2}$$

where $\mathbf{v}_i = (v_{0,1}^i, v_{1,1}^i, v_{1,2}^i, v_{1,3}^i,\ldots,v_{t,2t+1}^i)^\top\in\mathbb{R}^{d_t}$, which admit the following orthogonal property

$$\int_\Gamma S_i(\mathbf{x})S_j(\mathbf{x})d\omega(\mathbf{x}) = \lambda_i\delta_{ij} \text{ and } \int_{\mathbb{S}^2} S_i(\mathbf{x})S_j(\mathbf{x})d\omega(\mathbf{x}) = \delta_{ij},\ i,j=1,2,\ldots,d_t, \tag{2.3}$$

where $\delta_{ij}=1$, if $i=j$ and $\delta_{ij}=0$, if $i\neq j$.

The sum of the eigenvalues of $\mathbf{D}$ gives

$$S_h := \sum_{i=1}^{d_t}\lambda_i = \sum_{i=1}^{d_t}(\mathbf{D})_{i,i} = \sum_{\ell=0}^{t}\sum_{k=1}^{2\ell+1}\int_\Gamma Y_{\ell,k}^2(\mathbf{x})d\omega(\mathbf{x}) = \frac{|\Gamma|}{4\pi}d_t \tag{2.4}$$

the spherical Shannon number, which is a good estimate of the number of significant eigenvalues [25], where $|\Gamma|$ denotes the area of Γ.

Based on the well-known Funk-Hecke formula (see, for example, [5]) and Proposition 2.2 in [19], we obtain the following proposition on spherical zones.

PROPOSITION 2.1. *Let f be a continuous function on $[-1,1]$. For any $t\in\mathbb{N}_0$ and any $\mathbf{y}\in\mathbb{S}^2$, let $\mathbf{Y}_t^\rho(\mathbf{y}) = (\rho_0Y_{0,1}(\mathbf{y}), \rho_1Y_{1,1}(\mathbf{y}), \rho_1Y_{1,2}(\mathbf{y}),\ldots,\rho_tY_{t,2t+1}(\mathbf{y}))^\top$, where $\rho_i = 2\pi\int_{-1}^1 f(x)P_i(x)dx$, $i=0,1,\ldots,t$. For any fixed $\Theta = (\underline{\theta},\bar{\theta})^\top$ and $\ell\leq t$, we have*

$$\int_{\mathcal{Z}(\mathbf{e}_3;\Theta)} f(\mathbf{x}\cdot\mathbf{y})Y_{\ell,k}(\mathbf{x})d\omega(\mathbf{x}) = \mathbf{c}_{\ell,k}\mathbf{Y}_t^\rho(\mathbf{y}),\quad \forall\mathbf{y}\in\mathbb{S}^2, \tag{2.5}$$

where $\mathbf{c}_{\ell,k} := \mathbf{v}_{\ell,k}\Lambda\mathbf{V}^\top$, $\Lambda = \mathrm{diag}(\lambda_1,\ldots,\lambda_{d_t})$ and $\mathbf{V} = (\mathbf{v}_1,\ldots,\mathbf{v}_{d_t})$ with $\lambda_i,\mathbf{v}_i$ being the ith eigenvalue and corresponding eigenvector of the matrix $\mathbf{D}$ defined by (2.1) with $\Gamma = \mathcal{Z}(\mathbf{e}_3;\Theta)$, and $\mathbf{v}_{\ell,k}$ is the (ℓ^2+k)th row of the matrix $\mathbf{V}$.

The proof of Proposition 2.1 is similar with the proof of Proposition 2.2 in [19] by defining $\mathbf{D}$ on the spherical zone $\mathcal{Z}(\mathbf{e}_3;\Theta)$, and thus we omit it here. Besides, if $\underline{\theta}=0$ and $\bar{\theta}=\pi$, $\mathbf{D}$ is an identity matrix, and thus (2.5) reduces to the Funk-Hecke formula on the sphere. If $\underline{\theta}=0$ and $\bar{\theta}\neq\pi$, (2.5) reduces to Proposition 2.2 in [19].

3. Spherical zone t-designs. In this section, we first construct positive weight quadrature rules on spherical zones induced from quadrature rules on the unit sphere with polynomial exactness for spherical harmonics, product of spherical harmonics and a class of orthonormal functions on spherical zones. Then, we present spherical zone t-designs on spherical zones using spherical t-designs and trapezoidal rules (1.1) with polynomial exactness t on $[0,2\pi]$.

For convenience, for any $\Theta=(\underline{\theta},\bar{\theta})^\top$ with $0\leq\underline{\theta}<\bar{\theta}\leq\pi$, let

$$\kappa_1=\frac{2}{\cos\underline{\theta}-\cos\bar{\theta}}\quad\text{and}\quad\kappa_2=\frac{\cos\bar{\theta}+\cos\underline{\theta}}{\cos\underline{\theta}-\cos\bar{\theta}}.$$

For any $\Theta=(\underline{\theta},\bar{\theta})^\top$ with $0\leq\underline{\theta}<\bar{\theta}\leq\pi$ and $\mathbf{y}=(\sin\vartheta\cos\phi,\sin\vartheta\sin\phi,\cos\vartheta)^\top\in\mathbb{S}^2$, we define

$$\mathcal{R}(\mathbf{y};\Theta):=\begin{bmatrix}\cos^2\phi\cos\eta+\sin^2\phi & (\cos\eta-1)\cos\phi\sin\phi & -\cos\phi\sin\eta\\ (\cos\eta-1)\cos\phi\sin\phi & \sin^2\phi\cos\eta+\cos^2\phi & -\sin\phi\sin\eta\\ \cos\phi\sin\eta & \sin\phi\sin\eta & \cos\eta\end{bmatrix},\tag{3.1}$$

where $\eta:=\vartheta-\arccos((\cos\vartheta+\kappa_2)/\kappa_1)$.

Remark 3.1. By the definitions of κ_1 and κ_2, we have

$$(\cos\vartheta+\kappa_2)/\kappa_1=(\cos\vartheta(\cos\underline{\theta}-\cos\bar{\theta})+\cos\underline{\theta}+\cos\bar{\theta})/2\in[\cos\bar{\theta},\cos\underline{\theta}],\ \forall\vartheta\in[0,\pi].$$

Thus, $\vartheta-\eta=\arccos((\cos\vartheta+\kappa_2)/\kappa_1)\in[\underline{\theta},\bar{\theta}]$, $\forall\vartheta\in[0,\pi]$. Through matrix-vector multiplication and simplification, we obtain

$$\mathcal{R}(\mathbf{y};\Theta)\mathbf{y}=(\sin(\vartheta-\eta)\cos\phi,\sin(\vartheta-\eta)\sin\phi,\cos(\vartheta-\eta))^\top\in\mathcal{Z}(\mathbf{e}_3;\Theta),$$

for any $\mathbf{y}=(\sin\vartheta\cos\phi,\sin\vartheta\sin\phi,\cos\vartheta)^\top\in\mathbb{S}^2$.

By the rotational invariance of the unit sphere and Lemma 3.1 in [18], we show that it is sufficient to construct rules on the spherical zone $\mathcal{Z}(\mathbf{e}_3;\Theta)$ with center $\mathbf{e}_3$.

LEMMA 3.2. *If a quadrature rule on a spherical zone $\mathcal{Z}(\mathbf{e}_3;\Theta)$ with nodes $\mathcal{X}_n:=\{\mathbf{x}_1,\ldots,\mathbf{x}_n\}\subseteq\mathcal{Z}(\mathbf{e}_3;\Theta)$ and positive weights $w_1,\ldots,w_n$ has polynomial exactness $t\in\mathbb{N}_0$, that is,*

$$\int_{\mathcal{Z}(\mathbf{e}_3;\Theta)}P(\mathbf{x})d\omega(\mathbf{x})=\sum_{i=1}^n w_iP(\mathbf{x}_i),\quad\forall P\in\mathbb{P}_t(\mathbb{S}^2),\tag{3.2}$$

then

$$\int_{\mathcal{Z}(\mathbf{z};\Theta)}P(\mathbf{x})d\omega(\mathbf{x})=\sum_{i=1}^n w_iP(\mathbf{R}\mathbf{x}_i),\quad\forall P\in\mathbb{P}_t(\mathbb{S}^2),\tag{3.3}$$

where $\mathbf{R}\in\mathrm{SO}(3)$ is a rotation matrix such that $\mathbf{R}\mathbf{e}_3=\mathbf{z}$.

Proof. We see $\int_{\mathcal{Z}(\mathbf{z};\Theta)}P(\mathbf{x})d\omega(\mathbf{x})=\int_{\mathcal{Z}(\mathbf{e}_3;\Theta)}P(\mathbf{R}\mathbf{y})d\omega(\mathbf{y})=\sum_{i=1}^n w_iP(\mathbf{R}\mathbf{x}_i)$, where the first equality follows from $|\det(\mathbf{R})|=1$ and rotational invariance of the Lebesgue measure $d\omega(\mathbf{x})$, the last equality follows from (3.2). The proof is completed.□

3.1. Positive weight quadrature rules. Following the idea in [16, 19], we first present a set of real-valued orthonormal functions on a spherical zone $\mathcal{Z}(\mathbf{e}_3;\Theta)$ derived from a shifted Legendre polynomial of degree $\ell \in \mathbb{N}_0$ as follows,

$$\begin{aligned} T^{\kappa}_{\ell,1}(\theta,\phi) &= \sqrt{\kappa_1} N_{\ell,0} P_\ell(\kappa_1\cos\theta-\kappa_2),\\ T^{\kappa}_{\ell,2m}(\theta,\phi) &= \sqrt{\kappa_1} N_{\ell,m} P_{\ell,m}(\kappa_1\cos\theta-\kappa_2)\cos m\phi,\\ T^{\kappa}_{\ell,2m+1}(\theta,\phi) &= \sqrt{\kappa_1} N_{\ell,m} P_{\ell,m}(\kappa_1\cos\theta-\kappa_2)\sin m\phi,\ m=1,2,\ldots,\ell, \end{aligned}$$

for any $(\theta,\phi)\in[\underline{\theta},\bar{\theta}]\times[0,2\pi]$. For convenience, we write $T^{\kappa}_{\ell,k}(\mathbf{x}) := T^{\kappa}_{\ell,k}(\theta,\phi)$ with $\mathbf{x}=(\sin\theta\cos\phi,\sin\theta\sin\phi,\cos\theta)^\top \in \mathcal{Z}(\mathbf{e}_3;\Theta)$ for any $\ell\in\mathbb{N}_0$, $k\in\{1,\ldots,2\ell+1\}$.

The functions $\{T^{\kappa}_{\ell,k}\}$ are $\mathbb{L}_2(\mathcal{Z}(\mathbf{e}_3;\Theta))$-orthonormal to each other, that is,

$$\int_{\mathcal{Z}(\mathbf{e}_3;\Theta)} T^{\kappa}_{\ell,k}(\mathbf{x}) T^{\kappa}_{\ell',k'}(\mathbf{x}) d\omega(\mathbf{x}) = \delta_{\ell\ell'}\delta_{kk'}, \tag{3.4}$$

for any $\ell,\ell'\in\mathbb{N}_0, k\in\{1,\ldots,2\ell+1\}, k'\in\{1,\ldots,2\ell'+1\}$.

In the following, we present the relationship between $T^{\kappa}_{\ell,k}$ and $Y_{\ell,k}$. For notational simplicity, we define a function $\Upsilon:[\underline{\theta},\bar{\theta}]\to\mathbb{R}$ as follows

$$\Upsilon(\theta) = \begin{cases} 1 & \text{if } \underline{\theta}=0, \bar{\theta}=\pi\\ \kappa_1^2(\cos\theta-\cos\bar{\theta})/(1+\cos\theta) & \text{if } \underline{\theta}=0, \bar{\theta}\neq\pi\\ \kappa_1^2(\cos\theta-\cos\underline{\theta})/(1-\cos\theta) & \text{if } \underline{\theta}\neq 0, \bar{\theta}=\pi\\ (1-(\kappa_1\cos\theta-\kappa_2)^2)/(1-\cos^2\theta) & \text{otherwise.}\end{cases}$$

PROPOSITION 3.3. *Let $\underline{\theta}$, $\bar{\theta}$ satisfy $0\le\underline{\theta}<\bar{\theta}\le\pi$. Then for any $\ell\in\mathbb{N}_0$, $k\in\{1,\ldots,2\ell+1\}$ and any $(\theta,\phi)\in[\underline{\theta},\bar{\theta}]\times[0,2\pi]$, the following statements hold.*

(i) $T^{\kappa}_{\ell,k}(\theta,\phi)=\sqrt{\kappa_1}Y_{\ell,k}(\vartheta,\phi)$ with $\vartheta=\arccos(\kappa_1\cos\theta-\kappa_2)\in[0,\pi]$.

(ii)

$$(\Upsilon(\theta))^{\frac{\nu}{2}} Y_{\ell,k}(\theta,\phi) = \sum_{j=\nu}^{\ell}\beta_j T^{\kappa}_{j,k}(\theta,\phi), \tag{3.5}$$

where $\nu=\lfloor k/2\rfloor$, $\beta_j=\kappa_1^{\nu-0.5}a_jN_{\ell,\nu}/N_{j,\nu}$, $a_j=0.5\kappa_1(2j+1)\int_{\cos\bar{\theta}}^{\cos\underline{\theta}}P_\ell(x)P_j(\kappa_1x-\kappa_2)dx$, $j=\nu,\ldots,\ell$.

Proof. (i) follows from definitions of $T^{\kappa}_{\ell,k}$ and $Y_{\ell,k}$.

(ii) For any $\ell\in\mathbb{N}_0$, let

$$\begin{aligned} \psi^{\kappa}_{\ell,1}(\theta,\phi) &= \sqrt{\kappa_1}N_{\ell,0}P_\ell(\kappa_1\cos\theta-\kappa_2),\\ \psi^{\kappa}_{\ell,2m}(\theta,\phi) &= (-1)^m\sqrt{\kappa_1}N_{\ell,m}P^{(m)}_\ell(\kappa_1\cos\theta-\kappa_2)\sin^m\theta\cos m\phi,\\ \psi^{\kappa}_{\ell,2m+1}(\theta,\phi) &= (-1)^m\sqrt{\kappa_1}N_{\ell,m}P^{(m)}_\ell(\kappa_1\cos\theta-\kappa_2)\sin^m\theta\sin m\phi,\ m=1,\ldots,\ell, \end{aligned}$$

where $(\theta,\phi)\in[\underline{\theta},\bar{\theta}]\times[0,2\pi]$. Then following similar arguments as in the proof of Proposition 2.6 in [19], we obtain (ii). The proof is completed. ∎

Now, we introduce the induced quadrature rules on a spherical zone.

THEOREM 3.4. *If a quadrature rule on the unit sphere with quadrature nodes $\mathcal{Y}_n=\{\mathbf{y}_1,\ldots,\mathbf{y}_n\}\subset\mathbb{S}^2$ and positive weights $w_1,\ldots,w_n$ has polynomial exactness $t\in\mathbb{N}_0$, then*

$$\mathcal{X}^{\mathcal{Y}}_n := \{\mathbf{x}_j : \mathbf{x}_j=\mathcal{R}(\mathbf{y}_j;\Theta)\mathbf{y}_j, \mathbf{y}_j\in\mathcal{Y}_n, j=1,\ldots,n\}$$

is a set of points on $\mathcal{Z}(\mathbf{e}_3;\Theta)$ induced by $\mathcal{Y}_n$ such that the following statements hold.

(i) For any $\ell \le t$, $k \in \{1,2,\dots,2\ell+1\}$, we have

$$\int_{\mathcal{Z}(\mathbf{e}_3;\Theta)} T^{\kappa}_{\ell,k}(\mathbf{x})d\omega(\mathbf{x}) = \sum_{j=1}^{n} \frac{w_j}{\kappa_1} T^{\kappa}_{\ell,k}(\mathbf{x}_j).$$

(ii) For any $\ell \le t$, $k \in \{1,2,\dots,2\ell+1\}$, we have

$$\int_{\mathcal{Z}(\mathbf{e}_3;\Theta)} Y_{\ell,k}(\mathbf{x})d\omega(\mathbf{x}) = \sum_{j=1}^{n} \frac{w_j}{\kappa_1} (\Upsilon(\arccos(\mathbf{x}_j\cdot\mathbf{e}_3)))^{\frac{\lfloor k/2\rfloor}{2}} Y_{\ell,k}(\mathbf{x}_j).$$

(iii) For any $\ell,\ell' \in \mathbb{N}_0$ satisfying $2(\ell+\ell') \le t$, $k \in \{1,2,\dots,2\ell+1\}$,

$$\int_{\mathcal{Z}(\mathbf{e}_3;\Theta)} Y_{\ell,k}(\mathbf{x})Y_{\ell',k}(\mathbf{x})d\omega(\mathbf{x}) = \sum_{j=1}^{n} \frac{w_j}{\kappa_1} \sum_{\ell''=0}^{\ell+\ell'} c_{\ell'',1} Y_{\ell'',1}(\mathbf{x}_j),$$

where $c_{\ell'',1} = \sum_{i=1}^{n} w_i Y_{\ell,k}(\mathbf{y}_i)Y_{\ell',k}(\mathbf{y}_i)Y_{\ell'',1}(\mathbf{y}_i)$.

Proof. For any given Θ and $\mathbf{y}_j \in \mathcal{Y}_n$, by (3.1), we obtain $\mathbf{x}_j := \mathcal{R}(\mathbf{y}_j;\Theta)\mathbf{y}_j \in \mathcal{Z}(\mathbf{e}_3;\Theta)$, $j=1,\dots,n$, that is $\mathcal{X}_n^{\mathcal{Y}} \subseteq \mathcal{Z}(\mathbf{e}_3;\Theta)$. Then following similar arguments as in the proof of Lemma 3.1 in [19], we obtain (i).

(ii) For any $\ell \le t$ and $k \ne 1$, we have

$$\begin{aligned}\sum_{j=1}^{n} \frac{w_j}{\kappa_1} (\Upsilon(\arccos(\mathbf{x}_j\cdot\mathbf{e}_3)))^{\frac{\nu}{2}} Y_{\ell,k}(\mathbf{x}_j) &= \sum_{j=1}^{n} \frac{w_j}{\kappa_1} \sum_{i=\nu}^{\ell} \beta_i T^{\kappa}_{i,k}(\mathbf{x}_j) \\ &= \sum_{i=\nu}^{\ell} \beta_i \sum_{j=1}^{n} \frac{w_j}{\kappa_1} T^{\kappa}_{i,k}(\mathbf{x}_j) = 0 = \int_{\mathcal{Z}(\mathbf{e}_3;\Theta)} Y_{\ell,k}(\mathbf{x})d\omega(\mathbf{x}),\end{aligned} \tag{3.6}$$

where $\nu = \lfloor k/2\rfloor$, β_i are defined in Proposition 3.3, the first equality follows from (3.5), the third equality follows from (i) and the last equality follows from $\int_0^{2\pi} \cos m\phi d\phi = 0$ and $\int_0^{2\pi} \sin m\phi d\phi = 0$ for any integer $m \ne 0$.

For any $\ell \le t$ and $k = 1$, we have

$$\begin{aligned}\int_{\mathcal{Z}(\mathbf{e}_3;\Theta)} Y_{\ell,1}(\mathbf{x})d\omega(\mathbf{x}) &= \int_{\mathcal{Z}(\mathbf{e}_3;\Theta)} \sum_{i=0}^{\ell} \beta_i T^{\kappa}_{i,1}(\mathbf{x})d\omega(\mathbf{x}) \\ &= \sum_{j=1}^{n} \frac{w_j}{\kappa_1} \sum_{i=0}^{\ell} \beta_i T^{\kappa}_{i,1}(\mathbf{x}_j) = \sum_{j=1}^{n} \frac{w_j}{\kappa_1} Y_{\ell,1}(\mathbf{x}_j),\end{aligned}$$

where the first and the last equalities follow from (3.5) and the second equality follows from (i). Thus we obtain (ii).

(iii) It is easy to see that there are $c_{\ell'',k''} \in \mathbb{R}$ such that $Y_{\ell,k}(\mathbf{x})Y_{\ell',k}(\mathbf{x}) = \sum_{\ell''=0}^{\ell+\ell'} \sum_{k''=1}^{2\ell''+1} c_{\ell'',k''} Y_{\ell'',k''}(\mathbf{x})$, $\forall \mathbf{x} \in \mathbb{S}^2$. By (ii), for any ℓ,ℓ' satisfying $2(\ell+\ell') \le t$, we have

$$\begin{aligned}\int_{\mathcal{Z}(\mathbf{e}_3;\Theta)} Y_{\ell,k}(\mathbf{x})Y_{\ell',k}(\mathbf{x})d\omega(\mathbf{x}) &= \sum_{\ell''=0}^{\ell+\ell'} \sum_{k''=1}^{2\ell''+1} c_{\ell'',k''} \int_{\mathcal{Z}(\mathbf{e}_3;\Theta)} Y_{\ell'',k''}(\mathbf{x})d\omega(\mathbf{x}) \\ &= \sum_{\ell''=0}^{\ell+\ell'} c_{\ell'',1} \int_{\mathcal{Z}(\mathbf{e}_3;\Theta)} Y_{\ell'',1}(\mathbf{x})d\omega(\mathbf{x}) = \sum_{\ell''=0}^{\ell+\ell'} c_{\ell'',1} \sum_{j=1}^{n} \frac{w_j}{\kappa_1} Y_{\ell'',1}(\mathbf{x}_j),\end{aligned}$$

where the second equality follows from (3.6), the third equality follows from (ii) with $k = 1$. By definition of $\mathcal{Y}_n$, we have $c_{\ell'',1} = \int_{\mathbb{S}^2} Y_{\ell,k}(\mathbf{y}) Y_{\ell',k}(\mathbf{y}) Y_{\ell'',1}(\mathbf{y}) d\omega(\mathbf{y}) = \sum_{i=1}^n w_i Y_{\ell,k}(\mathbf{y}_i) Y_{\ell',k}(\mathbf{y}_i) Y_{\ell'',1}(\mathbf{y}_i)$. Hence we obtain (iii). The proof is completed. ∎

Remark 3.5. (Remark on Theorem 3.4) (i) If $\underline{\theta} = 0$ and $\bar{\theta} = \pi$, then $\mathcal{X}_n^{\mathcal{Y}} = \mathcal{Y}_n$. (ii) If $\mathcal{Y}_n$ is a spherical t-design, then: (a) Theorem 3.4(i) has equal weight $4\pi/(n\kappa_1)$ and $\sum_{j=1}^n \frac{4\pi}{n\kappa_1} = 2\pi(\cos\underline{\theta} - \cos\bar{\theta}) = |\mathcal{Z}(\mathbf{e}_3; \Theta)|$; (b) for $\underline{\theta} = 0$ and $\bar{\theta} \neq \pi$ (or $\underline{\theta} \neq 0$ and $\bar{\theta} = \pi$), $\mathcal{X}_n^{\mathcal{Y}}$ reduces to a spherical cap t-subdesign induced by the spherical t-design $\mathcal{Y}_n$, which has been studied in [19].

By Theorem 3.4(ii), we have the following results for spherical zonal polynomials.

THEOREM 3.6. *Let $\mathcal{Y}_n := \{\mathbf{y}_1, \ldots, \mathbf{y}_n\} \subset \mathbb{S}^2$ be a spherical t-design. Then,*

$$\mathcal{X}_n^{\mathcal{Y}} := \{\mathbf{x}_i : \mathbf{x}_i = \mathcal{R}(\mathbf{y}_i; \Theta)\mathbf{y}_i, \mathbf{y}_i \in \mathcal{Y}_n, i = 1, \ldots, n\} \tag{3.7}$$

provides an equal weight quadrature rule for spherical zonal polynomials of degree at most t on $\mathcal{Z}(\mathbf{e}_3; \Theta)$, that is,

$$\int_{\mathcal{Z}(\mathbf{e}_3;\Theta)} P(\mathbf{x}) d\omega(\mathbf{x}) = \frac{4\pi}{n\kappa_1} \sum_{i=1}^n P(\mathbf{x}_i) \tag{3.8}$$

holds for any zonal polynomial $P = \sum_{\ell=0}^t \alpha_{\ell,1} Y_{\ell,1} \in \mathbb{P}_t(\mathbb{S}^2)$, $\forall \alpha_{\ell,1} \in \mathbb{R}$.

The proof of Theorem 3.6 follows from Theorem 3.4(ii) by taking $k = 1$.

3.2. Spherical zone t-designs. In this section, we show the construction of spherical zone t-designs on a spherical zone $\mathcal{Z}(\mathbf{e}_3; \Theta)$.

THEOREM 3.7. *Let $\mathcal{Y}_n := \{\mathbf{y}_j \in \mathbb{S}^2 : \mathbf{y}_j = (\sin\vartheta_j \cos\phi_j, \sin\vartheta_j \sin\phi_j, \cos\vartheta_j)^\top, j = 1, \ldots, n\}$ be a spherical t-design and arbitrary $\zeta_j \in [0, 2\pi]$, $j = 1, \ldots, n$. Then,*

$$\begin{aligned} \mathcal{X}_{n(t+1)} := \Big\{ & \mathbf{x}_{ij} \in \mathcal{Z}(\mathbf{e}_3; \Theta) : \mathbf{x}_{ij} = (\sin\theta_j \cos\varphi_{ij}, \sin\theta_j \sin\varphi_{ij}, \cos\theta_j)^\top, \text{where} \\ & \theta_j = \arccos\Big(\frac{\cos\vartheta_j + \kappa_2}{\kappa_1}\Big),\ \varphi_{ij} = \left[\frac{2\pi(i-1)}{t+1} + \zeta_j\right]_{\mathrm{mod}2\pi}, \\ & j = 1, \ldots, n,\ i = 1, \ldots, t+1 \Big\} \end{aligned} \tag{3.9}$$

is a spherical zone t-design on the spherical zone $\mathcal{Z}(\mathbf{e}_3; \Theta)$, that is,

$$\int_{\mathcal{Z}(\mathbf{e}_3;\Theta)} P(\mathbf{x}) d\omega(\mathbf{x}) = \frac{4\pi}{n\kappa_1(t+1)} \sum_{j=1}^n \sum_{i=1}^{t+1} P(\mathbf{x}_{ij}), \quad \forall P \in \mathbb{P}_t(\mathbb{S}^2). \tag{3.10}$$

Proof. By the trapezoidal rule (1.1), for $j = 1, \ldots, n$ and any $m \leq t$, we have

$$\int_0^{2\pi} \cos m\varphi d\varphi = \frac{2\pi}{t+1} \sum_{i=1}^{t+1} \cos m\varphi_{ij} \text{ and } \int_0^{2\pi} \sin m\varphi d\varphi = \frac{2\pi}{t+1} \sum_{i=1}^{t+1} \sin m\varphi_{ij}. \tag{3.11}$$

It is sufficient to verify (3.10) for spherical harmonics $Y_{\ell,k}$ of degree $\leq t$. By Theorem 3.4(ii) and the definition of $Y_{\ell,1}$, for any $\ell \leq t$, we have

$$\int_{\underline{\theta}}^{\bar{\theta}} \int_0^{2\pi} Y_{\ell,1}(\theta, \varphi) \sin\theta d\theta d\varphi = \frac{4\pi}{n\kappa_1} \sum_{j=1}^n Y_{\ell,1}(\theta_j, \cdot) = \frac{4\pi}{n\kappa_1(t+1)} \sum_{j=1}^n \sum_{i=1}^{t+1} Y_{\ell,1}(\theta_j, \varphi_{ij}). \tag{3.12}$$

For any $\ell \le t$ and even k, let $m = k/2$, then we have

$$\begin{aligned}\frac{4\pi}{n\kappa_1(t+1)}\sum_{j=1}^{n}\sum_{i=1}^{t+1}Y_{\ell,k}(\mathbf{x}_{ij}) &= \frac{2N_{\ell,m}}{n\kappa_1}\sum_{j=1}^{n}P_{\ell,m}(\cos\theta_j)\left(\frac{2\pi}{t+1}\sum_{i=1}^{t+1}\cos m\varphi_{ij}\right)\\ &= \frac{2N_{\ell,m}}{n\kappa_1}\sum_{j=1}^{n}P_{\ell,m}(\cos\theta_j)\int_0^{2\pi}\cos m\varphi d\varphi = 0 = \int_{\mathcal{Z}(\mathbf{e}_3;\Theta)}Y_{\ell,k}(\mathbf{x})d\omega(\mathbf{x}),\end{aligned} \tag{3.13}$$

where the first equality follows from definition of $Y_{\ell,k}$ and the second equality follows from (3.11). Similarly, for any $\ell \le t$ and odd $k \ne 1$, $\frac{4\pi}{n\kappa_1(t+1)}\sum_{j=1}^{n}\sum_{i=1}^{t+1}Y_{\ell,k}(\mathbf{x}_{ij}) = \int_{\mathcal{Z}(\mathbf{e}_3;\Theta)}Y_{\ell,k}(\mathbf{x})d\omega(\mathbf{x})$. Then, combing (3.12) and (3.13), we complete the proof. ∎

Remark 3.8. (Remark on Theorem 3.7)

(i) If $\underline{\theta} = 0$ and $\bar{\theta} \ne \pi$, $\mathcal{X}_{n(t+1)}$ with $\kappa_1 = 2/(1-\cos\bar{\theta})$, $\kappa_2 = (1+\cos\bar{\theta})/(1-\cos\bar{\theta})$ in (3.9) is a spherical cap t-design. Similar result holds for $\underline{\theta} \ne 0$ and $\bar{\theta} = \pi$.

(ii) Let $\mathbf{R} \in \mathrm{SO}(3)\backslash\{\mathbf{I}\}$ be a rotation matrix such that $\mathbf{R}\mathbf{e}_3 = \mathbf{e}_3$. Then $\mathcal{X}'_{n(t+1)} := \{\mathbf{R}\mathbf{x}_{ij} \in \mathcal{Z}(\mathbf{e}_3;\Theta) : \mathbf{x}_{ij} \in \mathcal{X}_{n(t+1)}, j = 1,\dots,n, i = 1,\dots,t+1\}$ is also a spherical zone t-design on the spherical zone $\mathcal{Z}(\mathbf{e}_3;\Theta)$.

Remark 3.9. (Remark on the number of quadrature nodes) A lower bound [15] on the number of points of a spherical t-design is $\begin{cases}(t+1)(t+3)/4, & \text{if } t \text{ is odd}\\ (t+2)^2/4, & \text{if } t \text{ is even}\end{cases}$, which is achievable in a few special cases. The authors in [10] proved the existence of spherical t-designs with $\mathcal{O}(t^2)$ points, thus the spherical zone t-designs established in Theorem 3.7 with $\mathcal{O}(t^3)$ points exists. Chen et al. [11] established the existence of spherical t-designs for $t \le 100$ with $(t+1)^2$ points using the interval method, which implies that the spherical zone t-designs can have $(t+1)^3$ points for $t \le 100$. Following [31], we can obtain computed spherical zone t-designs with $t^2(t+1)/2 + \mathcal{O}(t^2)$ points. By Theorem 3.6, the number of quadrature nodes of the spherical zone t-designs for zonal polynomials coincides with that of spherical t-designs.

The sphere is invariant under rotations that any rotation of a spherical t-design is still a spherical t-design. In the following, we show a spherical zone 2-design with 6 points constructed based on a tight spherical 2-design which is rotated from the tight spherical 2-design

$$\mathcal{Y}_4^{\circ} := \left\{\begin{bmatrix}0\\0\\1\end{bmatrix}, \begin{bmatrix}\frac{\sqrt{8}}{3}\\0\\\frac{-1}{3}\end{bmatrix}, \begin{bmatrix}\frac{-\sqrt{2}}{3}\\\frac{\sqrt{6}}{3}\\\frac{-1}{3}\end{bmatrix}, \begin{bmatrix}\frac{-\sqrt{2}}{3}\\\frac{-\sqrt{6}}{3}\\\frac{-1}{3}\end{bmatrix}\right\}$$

given in [1]. The mesh norm and the separation distance of a point set $\mathcal{X}_n$ with respect to $\mathcal{Z}(\mathbf{e}_3;\Theta)$ are defined respectively by

$$h(\mathcal{X}_n) := \sup_{\mathbf{y}\in\mathcal{Z}(\mathbf{e}_3;\Theta)}\min_{\mathbf{x}_j\in\mathcal{X}_n}\mathrm{dist}(\mathbf{y},\mathbf{x}_j) \quad \text{and} \quad \tau(\mathcal{X}_n) := \min_{i\ne j}\mathrm{dist}(\mathbf{x}_i,\mathbf{x}_j),$$

where $\mathrm{dist}(\mathbf{x},\mathbf{y}) := \arccos(\mathbf{x}\cdot\mathbf{y})$, $\forall \mathbf{x}, \mathbf{y} \in \mathbb{S}^2$ is the geodesic distance.

Example 3.10. *Let $\mathcal{Y}_4$ be the spherical 2-design rotated from $\mathcal{Y}_4^{\circ}$, specifically,*

$$\mathcal{Y}_4 = \left\{\begin{bmatrix}0\\\frac{\sqrt{6}}{3}\\\frac{\sqrt{3}}{3}\end{bmatrix}, \begin{bmatrix}0\\\frac{-\sqrt{6}}{3}\\\frac{\sqrt{3}}{3}\end{bmatrix}, \begin{bmatrix}\frac{\sqrt{6}}{3}\\0\\\frac{-\sqrt{3}}{3}\end{bmatrix}, \begin{bmatrix}\frac{-\sqrt{6}}{3}\\0\\\frac{-\sqrt{3}}{3}\end{bmatrix}\right\}, \mathbf{R} = \begin{bmatrix}0 & 1 & 0\\\frac{\sqrt{3}}{3} & 0 & \frac{\sqrt{6}}{3}\\\frac{\sqrt{6}}{3} & 0 & \frac{\sqrt{3}}{3}\end{bmatrix},$$

where $\mathbf{R}$ *is the corresponding rotation matrix. We show* $\mathcal{Y}_4$ *in Fig.1(a).*

We choose a spherical zone $\mathcal{Z}(\mathbf{e}_3;\hat{\Theta})$ *with* $\hat{\Theta} = (\arccos\sqrt{3}/3, \arccos -\sqrt{3}/3)^\top$. *Thus,* $\kappa_1 = \sqrt{3}$ *and* $\kappa_2 = 0$.

By Theorems 3.4 and 3.6, the following set including four points

$$\mathcal{X}_4^{\mathcal{Y}} := \left\{ \begin{bmatrix} 0 \\ \frac{2\sqrt{2}}{3} \\ \frac{1}{3} \end{bmatrix}, \begin{bmatrix} 0 \\ \frac{-2\sqrt{2}}{3} \\ \frac{1}{3} \end{bmatrix}, \begin{bmatrix} \frac{2\sqrt{2}}{3} \\ 0 \\ \frac{-1}{3} \end{bmatrix}, \begin{bmatrix} \frac{-2\sqrt{2}}{3} \\ 0 \\ \frac{-1}{3} \end{bmatrix} \right\}$$

induced by $\mathcal{Y}_4$ *in Fig.1(b) provides equal weight quadrature rules for* $\{T_{\ell,k}^{\kappa}\}$ *for* $\ell \le 2$ *and spherical zonal polynomials of degree* ≤ 2.

Let $\mathcal{Q}_3^j := \{\varphi_{ij} = [2\pi(i-1)/3 + \zeta_j]_{\mathrm{mod}2\pi}, i = 1,2,3\}$, $j = 1,\ldots,4$.

By Theorem 3.7, we can obtain the following spherical zone 2*-designs on* $\mathcal{Z}(\mathbf{e}_3;\hat{\Theta})$.

(i) If $\zeta_1 = \zeta_2 = 0$ *and* $\zeta_3 = \zeta_4 = \pi/3$, *then we obtain a spherical zone* 2*-design with 6 points* $\mathcal{X}_6 = \{\mathbf{x}_1,\ldots,\mathbf{x}_6\}$, *see Fig.1(c), where*

$$\mathbf{x}_1 = \begin{bmatrix} \frac{2\sqrt{2}}{3} \\ 0 \\ \frac{1}{3} \end{bmatrix}, \mathbf{x}_2 = \begin{bmatrix} \frac{-\sqrt{2}}{3} \\ \frac{\sqrt{6}}{3} \\ \frac{1}{3} \end{bmatrix}, \mathbf{x}_3 = \begin{bmatrix} \frac{-\sqrt{2}}{3} \\ \frac{-\sqrt{6}}{3} \\ \frac{1}{3} \end{bmatrix}, \mathbf{x}_4 = -\mathbf{x}_3, \mathbf{x}_5 = -\mathbf{x}_1, \mathbf{x}_6 = -\mathbf{x}_2.$$

(ii) If $\zeta_j = 0$, $j = 1,\ldots,4$, *then we obtain a spherical zone* 2*-design with 6 points* $\hat{\mathcal{X}}_6 = \{\hat{\mathbf{x}}_1,\ldots,\hat{\mathbf{x}}_6\}$, *see Fig.1(d), where*

$$\hat{\mathbf{x}}_1 = \mathbf{x}_1, \hat{\mathbf{x}}_2 = \mathbf{x}_2, \hat{\mathbf{x}}_3 = \mathbf{x}_3, \hat{\mathbf{x}}_4 = \begin{bmatrix} \frac{2\sqrt{2}}{3} \\ 0 \\ \frac{-1}{3} \end{bmatrix}, \hat{\mathbf{x}}_5 = \begin{bmatrix} \frac{-\sqrt{2}}{3} \\ \frac{\sqrt{6}}{3} \\ \frac{-1}{3} \end{bmatrix}, \hat{\mathbf{x}}_6 = \begin{bmatrix} \frac{-\sqrt{2}}{3} \\ \frac{-\sqrt{6}}{3} \\ \frac{-1}{3} \end{bmatrix}.$$

In Fig. 1, the local mesh norm of spherical zone t*-designs is estimated by using a set of generalized spiral points [7] on the spherical zone* $\mathcal{Z}(\mathbf{e}_3;\hat{\Theta})$ *with 577,350 points.*

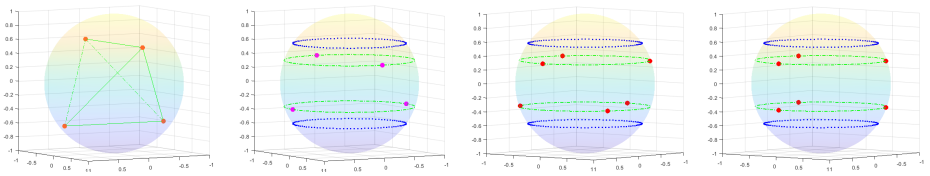

(a) $\mathcal{Y}_4$ (b) $\mathcal{X}_4^{\mathcal{Y}}$ (c) $\mathcal{X}_6$, $(0.9537, 1.2310)$ (d) $\hat{\mathcal{X}}_6$, $(1.0794, 0.6797)$

FIG. 1. *(a) spherical 2-design* $\mathcal{Y}_4$. *(b)* $\mathcal{X}_4^{\mathcal{Y}}$ *induced by* $\mathcal{Y}_4$. *(c) spherical zone 2-design* $\mathcal{X}_6$ *and (d) spherical zone 2-design* $\hat{\mathcal{X}}_6$, *where the dashed blue lines are the boundary of* $\mathcal{Z}(\mathbf{e}_3;\hat{\Theta})$ *and the pair* $(\cdot,\cdot)$ *is the estimated mesh norm and separation distance of* $\mathcal{X}_6$ *and* $\hat{\mathcal{X}}_6$, *respectively.*

We see from Example 3.10 that spherical t-designs having a symmetric property can significantly reduce the number of spherical zone t-designs. Spherical zone t-designs constructed with different ζ_j have better separation distance than using the same ζ_j. To further illustrate the above insight, we give another example in the following. We pesent a spherical zone 3-design with 8 points constructed from a symmetric spherical 3-design $\mathcal{Y}_6^{\circ} = \{\mathbf{e}_1, \mathbf{e}_2, \mathbf{e}_3, -\mathbf{e}_1, -\mathbf{e}_2, -\mathbf{e}_3\}$ given by [31], where $\mathbf{e}_1 = (1,0,0)^\top$ and $\mathbf{e}_2 = (0,1,0)^\top$.

EXAMPLE 3.11. *Let* $\mathcal{Z}(\mathbf{e}_3;\hat{\Theta})$ *with* $\hat{\Theta} = (\arccos\sqrt{3}/3, \arccos -\sqrt{3}/3)^\top$ *be a spherical zone, and* $\mathcal{Y}_6$ *(see Fig.2 (a)) be a symmetric spherical* 3*-design rotated from* $\mathcal{Y}_6^\circ$*, specifically*

$$\mathcal{Y}_6 = \left\{ \begin{bmatrix} 0 \\ \frac{\sqrt{6}}{3} \\ \frac{\sqrt{3}}{3} \end{bmatrix}, \begin{bmatrix} \frac{-\sqrt{2}}{2} \\ \frac{-\sqrt{6}}{6} \\ \frac{\sqrt{3}}{3} \end{bmatrix}, \begin{bmatrix} \frac{\sqrt{2}}{2} \\ \frac{-\sqrt{6}}{6} \\ \frac{\sqrt{3}}{3} \end{bmatrix}, \begin{bmatrix} 0 \\ \frac{-\sqrt{6}}{3} \\ \frac{-\sqrt{3}}{3} \end{bmatrix}, \begin{bmatrix} \frac{\sqrt{2}}{2} \\ \frac{\sqrt{6}}{6} \\ \frac{-\sqrt{3}}{3} \end{bmatrix}, \begin{bmatrix} \frac{-\sqrt{2}}{2} \\ \frac{\sqrt{6}}{6} \\ \frac{-\sqrt{3}}{3} \end{bmatrix} \right\}.$$

By Theorems 3.4 and 3.6, the induced point set $\mathcal{X}_6^{\mathcal{Y}}$ *(see Fig.2 (b)) is as follows*

$$\mathcal{X}_6^{\mathcal{Y}} = \left\{ \begin{bmatrix} 0 \\ \frac{\sqrt{8}}{3} \\ \frac{1}{3} \end{bmatrix}, \begin{bmatrix} \frac{-\sqrt{6}}{3} \\ \frac{-\sqrt{2}}{3} \\ \frac{1}{3} \end{bmatrix}, \begin{bmatrix} \frac{\sqrt{6}}{3} \\ \frac{-\sqrt{2}}{3} \\ \frac{1}{3} \end{bmatrix}, \begin{bmatrix} 0 \\ \frac{-\sqrt{8}}{3} \\ \frac{-1}{3} \end{bmatrix}, \begin{bmatrix} \frac{\sqrt{6}}{3} \\ \frac{\sqrt{2}}{3} \\ \frac{-1}{3} \end{bmatrix}, \begin{bmatrix} \frac{-\sqrt{6}}{3} \\ \frac{\sqrt{2}}{3} \\ \frac{-1}{3} \end{bmatrix} \right\}.$$

For $j = 1, \ldots, 6$*, let* $\mathcal{Q}_4^j := \{\varphi_{ij} = [2\pi(i-1)/4 + \zeta_j]_{\mathrm{mod}2\pi}, i = 1, 2, 3, 4\}$*, where* $\zeta_1 = \zeta_2 = \zeta_3 = 0$ *and* $\zeta_4 = \zeta_5 = \zeta_6 = \pi/4$*. By Theorem 3.7, we obtain a spherical zone* 3*-design* $\mathcal{X}_8$ *(see Fig.2 (c)) with* 8 *points, specifically,*

$$\mathcal{X}_8 = \{\mathbf{x}_1, \mathbf{x}_2, \mathbf{x}_3, \mathbf{x}_4, \mathbf{x}_5, \mathbf{x}_6, \mathbf{x}_7, \mathbf{x}_8\} =$$
$$\left\{ \begin{bmatrix} \frac{\sqrt{8}}{3} \\ 0 \\ \frac{1}{3} \end{bmatrix}, \begin{bmatrix} 0 \\ \frac{\sqrt{8}}{3} \\ \frac{1}{3} \end{bmatrix}, \begin{bmatrix} \frac{-\sqrt{8}}{3} \\ 0 \\ \frac{1}{3} \end{bmatrix}, \begin{bmatrix} 0 \\ \frac{-\sqrt{8}}{3} \\ \frac{1}{3} \end{bmatrix}, \begin{bmatrix} \frac{2}{3} \\ \frac{2}{3} \\ \frac{-1}{3} \end{bmatrix}, \begin{bmatrix} \frac{-2}{3} \\ \frac{2}{3} \\ \frac{-1}{3} \end{bmatrix}, \begin{bmatrix} \frac{-2}{3} \\ \frac{-2}{3} \\ \frac{-1}{3} \end{bmatrix}, \begin{bmatrix} \frac{2}{3} \\ \frac{-2}{3} \\ \frac{-1}{3} \end{bmatrix} \right\}.$$

We show the spherical zone 3-design $\hat{\mathcal{X}}_8 = \{\mathbf{x}_1, \mathbf{x}_2, \mathbf{x}_3, \mathbf{x}_4, -\mathbf{x}_1, -\mathbf{x}_2, -\mathbf{x}_3, -\mathbf{x}_4\}$ *constructed by choosing* $\zeta_1 = \ldots = \zeta_6 = 0$ *in Fig.2 (d).*

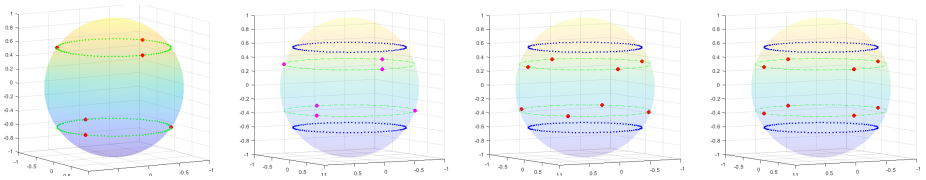

(a) $\mathcal{Y}_6$ (b) $\mathcal{X}_6^{\mathcal{Y}}$ (c) $\mathcal{X}_8$, (0.7424,1.0270) (d) $\hat{\mathcal{X}}_8$, (0.8402,0.6797)

FIG. 2. *(a) symmetric spherical 3-design* $\mathcal{Y}_6$*. (b)* $\mathcal{X}_6^{\mathcal{Y}}$ *induced by* $\mathcal{Y}_6$*. (C) spherical zone 3-design* $\mathcal{X}_8$ *and (d) spherical zone 3-design* $\hat{\mathcal{X}}_8$*, where the dashed blue lines are the boundary of* $\mathcal{Z}(\mathbf{e}_3;\hat{\Theta})$ *and the pair* $(\cdot,\cdot)$ *is the estimated mesh norm and separation distance of* $\mathcal{X}_8$*, respectively.*

In [18], the authors show the construction of spherical cap t-designs with $O(t^3)$ points based on equal weight rules on $[-1, 1]$ due to Bernstein [8]. In the following, we show an alternative construction of spherical zone t-designs on spherical zones using the method in [18].

LEMMA 3.12. *([8]) Let* t *be a positive odd integer, that is,* $t = 2k - 1$ *with a suitable* $k \in \mathbb{N}_0$*, and let* M *be an even integer such that* $M \geq M_0(t) := 2\lfloor\sqrt{2}(t + 3)(t + 9)/2 + 1\rfloor = 2\lfloor 2\sqrt{2}(r + 1)(r + 4) + 1\rfloor$*. There exist nodes* $x_1 > x_2 > \ldots > x_t$ *in* $(-1, 1)$ *and weights* $s_1, s_2, \ldots, s_t$ *such that (i)* $x_{2k-i} = -x_i$ *for* $i = 1, \ldots, t$*, (ii)* s_i*,* $i = 1, \ldots, t$ *are positive integers, (iii)* $s_i = s_{2k-i}$ *for* $i = 1, \ldots, t$*, (iv)* $\sum_{i=1}^t s_i = M$*, and (v) the numerical integration rule* $\int_{-1}^1 P(x)dx = \frac{2}{M}\sum_{i=1}^t s_i P(x_i)$ *holds for any polynomial* $P \in \mathbb{P}_t([-1, 1])$*.*

COROLLARY 3.13. *Let t be a positive odd integer, the set $\{(\frac{2s_j}{M}, x_j) : \sum_{j=1}^{t} s_j = M, s_j \in \mathbb{N}_0 \setminus \{0\}, x_j \in [-1,1],\ j = 1,\dots,t\}$ satisfy Lemma 3.12, and let $\zeta_j \in [0, 2\pi]$ be arbitrary for $j = 1,\dots,n$. Then*

$$\mathcal{X}_{M(t+1)} := \Bigg\{ \mathbf{x}_{ij} \in \mathcal{Z}(\mathbf{e}_3;\Theta) : \mathbf{x}_{ij} = (\sin\theta_j \cos\varphi_{ij}, \sin\theta_j \sin\varphi_{ij}, \cos\theta_j)^\top, \\ \text{where } \theta_j = \arccos\Big(\frac{x_j + \kappa_2}{\kappa_1}\Big),\ \varphi_{ij} = \Big[\frac{2\pi(i-1)}{(t+1)s_j} + \zeta_j\Big]_{\mathrm{mod}2\pi}, \\ i = 1, 2, \dots, (t+1)s_j,\ j = 1, 2, \dots, t \Bigg\} \tag{3.14}$$

is a spherical zone t-design on $\mathcal{Z}(\mathbf{e}_3;\Theta)$, that is,

$$\int_{\mathcal{Z}(\mathbf{e}_3;\Theta)} P(\mathbf{x}) d\omega(\mathbf{x}) = \frac{4\pi}{\kappa_1 (t+1) M} \sum_{j=1}^{t} \sum_{i=1}^{(t+1)s_j} P(\mathbf{x}_{ij}), \quad \forall P \in \mathbb{P}_t(\mathbb{S}^2). \tag{3.15}$$

The proof of Corollary 3.13 is similar with the proof of Theorem 3.7, thus we omit it here. Notice that the rule in Corollary 3.13 holds for $t-1$.

Remark 3.14. (Remark on Corollary 3.13) Different from [18], we choose $\{\zeta_j\}_{j=1}^n$ in (3.14) such that $\mathcal{X}_{M(t+1)}$ has relatively better separation distance. As stated in [18], the number of nodes in (3.14) is bounded by $2(t+1)\lfloor (t+3)(t+9)/\sqrt{2} + 1 \rfloor$ which is more than the number of nodes in (3.9). Thus, we take Corollary 3.13 as an alternative method for constructing equal weight quadrature rules on a spherical zone and will not discuss it in detail in this paper.

In the following, we present an error bound for numerical integration of continuous functions on a spherical zone $\mathcal{Z}(\mathbf{e}_3;\Theta)$ using spherical zone t-designs constructed above. We denote $E_t(f) := \inf_{P \in \mathbb{P}_t(\mathcal{Z}(\mathbf{e}_3;\Theta))} \|f - P\|_{\mathbb{L}_\infty(\mathcal{Z}(\mathbf{e}_3;\Theta))}$.

THEOREM 3.15. *Let $t \in \mathbb{N}_0$ and $\mathcal{X}_n := \{\mathbf{x}_1, \dots, \mathbf{x}_n\}$ be a spherical zone t-design on a spherical zone $\mathcal{Z}(\mathbf{e}_3;\Theta)$. Given $f \in \mathbb{C}(\mathcal{Z}(\mathbf{e}_3;\Theta))$, we have*

$$\Big| \frac{4\pi}{n\kappa_1} \sum_{i=1}^{n} f(\mathbf{x}_i) - \int_{\mathcal{Z}(\mathbf{e}_3;\Theta)} f(\mathbf{x}) d\omega(\mathbf{x}) \Big| \le \frac{8\pi}{\kappa_1} E_t(f).$$

Proof. We first observe that $\frac{4\pi}{n\kappa_1} \sum_{i=1}^{n} P(\mathbf{x}_i) = \int_{\mathcal{Z}(\mathbf{e}_3;\Theta)} P(\mathbf{x}) d\omega(\mathbf{x})$ for any $P \in \mathbb{P}_t(\mathcal{Z}(\mathbf{e}_3;\Theta))$. Then, for any $P \in \mathbb{P}_t(\mathcal{Z}(\mathbf{e}_3;\Theta))$, we have

$$\begin{aligned} &\Big| \tfrac{4\pi}{n\kappa_1} \textstyle\sum_{i=1}^{n} f(\mathbf{x}_i) - \int_{\mathcal{Z}(\mathbf{e}_3;\Theta)} f(\mathbf{x}) d\omega(\mathbf{x}) \Big| \\ =& \Big| \tfrac{4\pi}{n\kappa_1} \textstyle\sum_{i=1}^{n} (f(\mathbf{x}_i) - P(\mathbf{x}_i)) + \int_{\mathcal{Z}(\mathbf{e}_3;\Theta)} P(\mathbf{x}) - f(\mathbf{x}) d\omega(\mathbf{x}) \Big| \\ \le& \tfrac{4\pi}{n\kappa_1} \textstyle\sum_{i=1}^{n} |f(\mathbf{x}_i) - P(\mathbf{x}_i)| + \int_{\mathcal{Z}(\mathbf{e}_3;\Theta)} |P(\mathbf{x}) - f(\mathbf{x})| d\omega(\mathbf{x}) \\ \le& \tfrac{4\pi}{\kappa_1} \|f - P\|_{\mathbb{L}_\infty(\mathcal{Z}(\mathbf{e}_3;\Theta))} + \sqrt{\tfrac{4\pi}{\kappa_1}} \|P - f\|_{\mathbb{L}_2(\mathcal{Z}(\mathbf{e}_3;\Theta))} \le \tfrac{8\pi}{\kappa_1} E_t(f), \end{aligned}$$

where the second inequality follows from Cauchy–Schwarz inequality and the last inequality follows from arbitrariness of $P \in \mathbb{P}_t(\mathcal{Z}(\mathbf{e}_3;\Theta))$. The proof is completed. ∎

4. Approximation on spherical zones. In this section, we consider approximations using spherical zone t-designs and Slepian functions on a spherical zone.

For convenience, for any $t \in \mathbb{N}_0$, let $\mathbf{D} \in \mathbb{R}^{d_t \times d_t}$ be the positive definite matrix defined as (2.1) with $\Gamma = \mathcal{Z}(\mathbf{e}_3; \Theta)$ and spherical Shannon number $S_h := |\Gamma| d_t/(4\pi)$. We observe that $(\mathbf{D})_{\ell^2+k,\ell'^2+k'} = 0$ for $k \neq k'$, thus we apply the quadrature rules in section 3 to discretize the elements in $\mathbf{D}$ and denote the eigenvalues and corresponding eigenvectors of $\mathbf{D}$ by $\lambda_i, \mathbf{v}_i$, $i = 1, \ldots, d_t$, respectively. Then, we denote by $\{S_i\}_{i=1}^{d_t}$ the Slepian functions on $\mathcal{Z}(\mathbf{e}_3; \Theta)$ defined following (2.2).

4.1. Hyperinterpolation on spherical zones. Hyperinterpolation [26] is a discretization of the $\mathbb{L}_2$ orthogonal projection of a continuous function f on the sphere onto $\mathbb{P}_t(\mathbb{S}^2)$ by a quadrature rule with polynomial exactness $2t$. In this section, we study hyperinterpolation on a spherical zone. We consider the approximation of a continuous function f on a spherical zone $\mathcal{Z}(\mathbf{e}_3; \Theta)$ using Slepian functions and spherical zone t-designs and present an error bound in $\mathbb{L}_2$ norm.

THEOREM 4.1. *Let $t \in \mathbb{N}_0$ and $\mathcal{X}_n := \{\mathbf{x}_1, \ldots, \mathbf{x}_n\}$ be a spherical zone $2t$-design on the spherical zone $\mathcal{Z}(\mathbf{e}_3; \Theta)$. Given $f \in \mathbb{C}(\mathcal{Z}(\mathbf{e}_3; \Theta))$, let*

$$\mathcal{H}_t f := \frac{4\pi}{n\kappa_1} \sum_{j=1}^{d_t} \frac{1}{\lambda_j} \sum_{i=1}^{n} f(\mathbf{x}_i) S_j(\mathbf{x}_i) S_j.$$

Then the following statements hold.

(i) $\sum_{i=1}^{n} (\mathcal{H}_t f(\mathbf{x}_i))^2 \leq \sum_{i=1}^{n} f^2(\mathbf{x}_i)$.

(ii) $\|\mathcal{H}_t f\|_{\mathbb{L}_2(\mathcal{Z}(\mathbf{e}_3;\Theta))} \leq \sqrt{4\pi/\kappa_1} \|f\|_{\mathbb{L}_\infty(\mathcal{Z}(\mathbf{e}_3;\Theta))}$.

(iii) $\|\mathcal{H}_t f - f\|_{\mathbb{L}_2(\mathcal{Z}(\mathbf{e}_3;\Theta))} \leq 2\sqrt{4\pi/\kappa_1} E_t(f)$.

Proof. (i) Let $\langle f, g \rangle_n := \frac{4\pi}{n\kappa_1} \sum_{i=1}^{n} f(\mathbf{x}_i) g(\mathbf{x}_i)$, $\forall f, g \in \mathbb{C}(\mathcal{Z}(\mathbf{e}_3; \Theta))$. Then,

$$\langle \mathcal{H}_t f, S_j \rangle_n = \langle \sum_{i=1}^{d_t} \frac{\langle f, S_i \rangle_n}{\lambda_i} S_i, S_j \rangle_n = \sum_{i=1}^{d_t} \frac{\langle f, S_i \rangle_n}{\lambda_i} \langle S_i, S_j \rangle_n = \langle f, S_j \rangle_n, \ j = 1, \ldots, d_t,$$

where the last equality follows from exactness of spherical zone $2t$-design and orthogonality of Slepian functions, that is, $\langle S_i, S_j \rangle_n = \int_{\mathcal{Z}(\mathbf{e}_3;\Theta)} S_i(\mathbf{x}) S_j(\mathbf{x}) d\omega(\mathbf{x}) = \lambda_i \delta_{ij}$. Thus, we obtain $\langle \mathcal{H}_t f, \mathcal{H}_t f \rangle_n = \langle f, \mathcal{H}_t f \rangle_n$. Then, we have

$$\langle f - \mathcal{H}_t f, f - \mathcal{H}_t f \rangle_n = \langle f, f \rangle_n + \langle \mathcal{H}_t f, \mathcal{H}_t f \rangle_n - 2\langle f, \mathcal{H}_t f \rangle_n = \langle f, f \rangle_n - \langle \mathcal{H}_t f, \mathcal{H}_t f \rangle_n,$$

which implies $\langle \mathcal{H}_t f, \mathcal{H}_t f \rangle_n \leq \langle f, f \rangle_n$ due to $\langle f - \mathcal{H}_t f, f - \mathcal{H}_t f \rangle_n \geq 0$. We obtain (i).

(ii) It is easy to see that

$$\|\mathcal{H}_t f\|^2_{\mathbb{L}_2(\mathcal{Z}(\mathbf{e}_3;\Theta))} = \frac{4\pi}{n\kappa_1} \sum_{i=1}^{n} (\mathcal{H}_t f(\mathbf{x}_i))^2 \leq \frac{4\pi}{n\kappa_1} \sum_{i=1}^{n} f^2(\mathbf{x}_i) \leq \frac{4\pi}{\kappa_1} \|f\|^2_{\mathbb{L}_\infty(\mathcal{Z}(\mathbf{e}_3;\Theta))}.$$

Hence, (ii) holds.

(iii) For any $P \in \mathbb{P}_t(\mathcal{Z}(\mathbf{e}_3; \Theta))$, we have $\mathcal{H}_t P = P$. Thus, we obtain

$$\begin{aligned} &\|\mathcal{H}_t f - f\|_{\mathbb{L}_2(\mathcal{Z}(\mathbf{e}_3;\Theta))} = \|\mathcal{H}_t f + P - P - f\|_{\mathbb{L}_2(\mathcal{Z}(\mathbf{e}_3;\Theta))} \\ &\leq \|P - f\|_{\mathbb{L}_2(\mathcal{Z}(\mathbf{e}_3;\Theta))} + \|\mathcal{H}_t(f - P)\|_{\mathbb{L}_2(\mathcal{Z}(\mathbf{e}_3;\Theta))} \leq \sqrt{\tfrac{16\pi}{\kappa_1}} \|P - f\|_{\mathbb{L}_\infty(\mathcal{Z}(\mathbf{e}_3;\Theta))}. \end{aligned}$$

By the arbitrariness of $P \in \mathbb{P}_t(\mathcal{Z}(\mathbf{e}_3; \Theta))$, we obtain (iii). The proof is completed. ∎

4.2. Sparse approximation on spherical zones. In this subsection, we consider the sparse approximation of a continuous function from noisy data on $\mathcal{Z}(\mathbf{e}_3;\Theta)$. Let $\mathcal{X}_n := \{\mathbf{x}_1,\ldots,\mathbf{x}_n\}$ be a spherical zone $2t$-design on a spherical zone $\mathcal{Z}(\mathbf{e}_3;\Theta)$. We apply the following capped-l_1 optimization model to approximate a continuous function f from noise perturbed data at $\mathcal{X}_n = \{\mathbf{x}_1,\ldots,\mathbf{x}_n\}$,

$$\min_{\mathbf{u}\in\mathbb{R}^d} \quad F(\mathbf{u}) := \frac{1}{2}\|\mathbf{A}\mathbf{u}-\mathbf{b}\|^2 + \mu\sum_{i=1}^{d}\min\left(\frac{|u_i|}{\delta},1\right), \tag{4.1}$$

where $\mathbf{b} = \bar{w}(\mathbf{f}+\boldsymbol{\epsilon})$ with $\mathbf{f} = (f(\mathbf{x}_1),\ldots,f(\mathbf{x}_n))^\top$ and $\boldsymbol{\epsilon} = (\epsilon_1,\ldots,\epsilon_n)^\top$ is a noisy vector, $\bar{w} = \sqrt{4\pi/(n\kappa_1)}$, $\mathbf{A}\in\mathbb{R}^{n\times d}$ is a matrix with elements $(\mathbf{A})_{i,j} = \bar{w}S_j(\mathbf{x}_i)$, $i=1,\ldots,n$, $j=1,\ldots,d$, $\{S_i\}_{i=1}^d$ are the first $d := \lceil |\mathcal{Z}(\mathbf{e}_3;\Theta)|d_t/(4\pi)\rceil \le d_t$ optimally concentrated [25] Slepian functions on $\mathcal{Z}(\mathbf{e}_3;\Theta)$, $\mu>0$ and $\delta>0$.

Since $\mathcal{X}_n$ is a spherical zone $2t$-design, we have $\mathbf{A}^\top\mathbf{A} = \Lambda := \mathrm{diag}\{\lambda_1,\ldots,\lambda_d\}$. Let $g(\mathbf{u}) := \frac{1}{2}\|\mathbf{A}\mathbf{u}-\mathbf{b}\|^2$. Then $g:\mathbb{R}^d\to\mathbb{R}$ is strongly convex.

Now, we consider directional stationary points (see, for example, [17, 23]) of problem (4.1). The directional derivative of F at $\mathbf{u} = (u_1,\ldots,u_d)^\top$ along a direction $\mathbf{h}$ is defined by (see, for example, [17])

$$\begin{aligned} F'(\mathbf{u};\mathbf{h}) :&= \lim_{\tau\downarrow 0}\frac{F(\mathbf{u}+\tau\mathbf{h})-F(\mathbf{u})}{\tau} \\ &= \nabla g(\mathbf{u})^\top\mathbf{h} + \frac{\mu}{\delta}\Big(\sum_{i\in\mathcal{I}_<^\delta(\mathbf{u})}\mathrm{sign}(u_i)h_i + \sum_{i\in\mathcal{I}_=^\delta(\mathbf{u})}\min\{\mathrm{sign}(u_i)h_i,0\} + \sum_{i\in\mathcal{I}_0(\mathbf{u})}|h_i|\Big), \end{aligned}$$

where $\mathcal{I}_<^\delta(\mathbf{u}) := \{i: 0<|u_i|<\delta\}$, $\mathcal{I}_=^\delta(\mathbf{u}) := \{i:|u_i|=\delta\}$, and $\mathcal{I}_0(\mathbf{u}) := \{i:u_i=0\}$.

Definition 4.2. *We call $\mathbf{u}^*\in\mathbb{R}^d$ a directional stationary point of (4.1) if*

$$F'(\mathbf{u}^*;\mathbf{u}-\mathbf{u}^*)\ge 0,\ \forall\mathbf{u}\in\mathbb{R}^d.$$

By the discussions in [9, 17, 23], we obtain the following lower bounded property of directional stationary points of (4.1) and optimality conditions of problem (4.1).

Theorem 4.3. *Assume that $\delta \le \frac{\mu}{\|\mathbf{A}^\top\mathbf{b}\|_\infty}$. Then the following statements hold.*

(i) If $\mathbf{u}^*\in\mathbb{R}^d$ is a directional stationary point of (4.1), then, for every $i=1,\ldots,d$,

$$\textit{either}\quad u_i^* = 0 \quad \textit{or}\quad |u_i^*|>\delta.$$

Moreover, $u_i^* = \lambda_i^{-1}(\mathbf{A}^\top\mathbf{b})_i$, if $u_i^*\neq 0$.

(ii) $\mathbf{u}^*\in\mathbb{R}^d$ is a directional stationary point of (4.1) if and only if $F(\mathbf{u}^*)\le F(\mathbf{u})$, $\forall\mathbf{u}\in\mathcal{N}(\mathbf{u}^*)$, where

$$\mathcal{N}(\mathbf{u}^*) = \left\{\mathbf{u}\in\mathbb{R}^d : u_i\in\begin{cases}[-\delta,\delta] & \text{if } u_i^*=0\\ [\delta,u_i^*+\delta] & \text{if } u_i^*>\delta\\ [u_i^*-\delta,-\delta] & \text{if } u_i^*<-\delta\end{cases}\right\}.$$

Proof. (i) Assume on the contrary that there is $i\in\mathcal{I}_<^\delta(\mathbf{u}^*)\cup\mathcal{I}_=^\delta(\mathbf{u}^*)$. If $i\in\mathcal{I}_<^\delta(\mathbf{u}^*)$, then

$$\lambda_i u_i^* - (\mathbf{A}^\top\mathbf{b})_i + \frac{\mu}{\delta}\mathrm{sign}(u_i^*) \le \lambda_i u_i^* - (\mathbf{A}^\top\mathbf{b})_i - \|\mathbf{A}^\top\mathbf{b}\|_\infty < 0, \quad \text{if } u_i^*<0,$$

$$\lambda_i u_i^* - (\mathbf{A}^\top\mathbf{b})_i + \frac{\mu}{\delta}\mathrm{sign}(u_i^*) \ge \lambda_i u_i^* - (\mathbf{A}^\top\mathbf{b})_i + \|\mathbf{A}^\top\mathbf{b}\|_\infty > 0, \quad \text{if } u_i^*>0,$$

which is in contradiction to $(\lambda_i u_i^* - (\mathbf{A}^\top \mathbf{b})_i + \frac{\mu}{\delta}\operatorname{sign}(u_i^*))(u_i - u_i^*) \geq 0$, $\forall u_i \in \mathbb{R}$. If $i \in \mathcal{I}_=^\delta(\mathbf{u}^*)$, then

$$\lambda_i u_i^* - (\mathbf{A}^\top \mathbf{b})_i + \frac{\mu}{\delta}\min\{\operatorname{sign}(u_i^*), 0\} \geq 0,$$

$$-(\lambda_i u_i^* - (\mathbf{A}^\top \mathbf{b})_i) + \frac{\mu}{\delta}\min\{-\operatorname{sign}(u_i^*), 0\} \geq 0,$$

which imply $\min\{-\operatorname{sign}(u_i^*), 0\} + \min\{\operatorname{sign}(u_i^*), 0\} \geq 0$. Obviously, this inequality does not hold for $|u_i^*| = \delta$. Thus, the set $\mathcal{I}_<^\delta(\mathbf{u}^*) \cup \mathcal{I}_=^\delta(\mathbf{u}^*)$ is empty.

For any $i \in \mathcal{I}_>^\delta(\mathbf{u}^*) := \{i : |u_i^*| > \delta\}$, we have $(\lambda_i u_i^* - (\mathbf{A}^\top \mathbf{b})_i)(u_i - u_i^*) \geq 0$, $\forall u_i \in \mathbb{R}$ which implies $\lambda_i u_i^* - (\mathbf{A}^\top \mathbf{b})_i = 0$, and thus $u_i^* = \lambda_i^{-1}(\mathbf{A}^\top \mathbf{b})_i$.

(ii) If $F(\mathbf{u}^*) \leq F(\mathbf{u})$, $\forall \mathbf{u} \in \mathcal{N}(\mathbf{u}^*)$, then $\mathbf{u}^*$ is a local minimizer of (4.1). Hence it is a directional stationary point of (4.1).

Let $\mathbf{u}^*$ be a directional stationary point of (4.1). Then for any $\mathbf{u} \in \mathcal{N}(\mathbf{u}^*)$, we have

$$\begin{aligned}
&F(\mathbf{u}) - F(\mathbf{u}^*) - F'(\mathbf{u}^*; \mathbf{u} - \mathbf{u}^*) \\
&\geq \frac{\mu}{\delta}\Big(\sum_{i=1}^d \min(|u_i|, \delta) - \sum_{i=1}^d \min(|u_i^*|, \delta) - \sum_{i \in \mathcal{I}_0(\mathbf{u}^*)} |u_i|\Big) \\
&= \frac{\mu}{\delta}\Big(\sum_{i \in \mathcal{I}_0(\mathbf{u}^*)} \min(|u_i|, \delta) + \sum_{i \notin \mathcal{I}_0(\mathbf{u}^*)} \min(|u_i|, \delta) - \sum_{i \notin \mathcal{I}_0(\mathbf{u}^*)} \delta - \sum_{i \in \mathcal{I}_0(\mathbf{u}^*)} |u_i|\Big) = 0,
\end{aligned}$$

where the first inequality follows from definitions of F and $F'(\mathbf{u}^*; \mathbf{u} - \mathbf{u}^*)$, convexity of g, that is, $g(\mathbf{u}) - g(\mathbf{u}^*) \geq \nabla g(\mathbf{u}^*)^\top(\mathbf{u} - \mathbf{u}^*)$ and (i), the first equality follows from (i), the last equality follows from definition of $\mathcal{N}(\mathbf{u}^*)$. Thus, $F(\mathbf{u}) - F(\mathbf{u}^*) \geq F'(\mathbf{u}^*; \mathbf{u} - \mathbf{u}^*) \geq 0$ for any $\mathbf{u} \in \mathcal{N}(\mathbf{u}^*)$ and $\mathbf{u}^*$ is a local minimizer of (4.1). The proof is completed. ∎

From [9], we know that any local minimizer of problem (4.1) is a local minimizer of the cardinality constrained problem: $\min \frac{1}{2}\|\mathbf{A}\mathbf{u} - \mathbf{b}\|^2 + \mu\|\mathbf{u}\|_0$. Moreover, any global minimizer of the cardinality constrained problem is a global minimizer of problem (4.1). We shall refer to [9, 17] for comprehensive discussions.

Now, we estimate the approximation error in the $\mathbb{L}_2$ norm.

THEOREM 4.4. *Assume that $\delta \leq \frac{\mu}{\|\mathbf{A}^\top \mathbf{b}\|_\infty}$. Let $\mathbf{u}^* = (u_1^*, \ldots, u_d^*)^\top$ be a directional stationary point of problem (4.1) and $\mathcal{H}_t^* f = \sum_{i=1}^d u_i^* S_i$. Then,*

$$\|\mathcal{H}_t^* f - f\|_{\mathbb{L}_2(\mathcal{Z}(\mathbf{e}_3;\Theta))} \leq \sqrt{\frac{4\pi\|\mathbf{u}^*\|_0}{n\kappa_1}}\|\boldsymbol{\epsilon}\| + \sqrt{\frac{8\pi}{\kappa_1}}\|f\|_{\mathbb{L}_\infty(\mathcal{Z}(\mathbf{e}_3;\Theta))} + \sqrt{\frac{16\pi}{\kappa_1}}E_t(f). \tag{4.2}$$

Proof. For notational simplicity, we write $\mathbb{L}_2 := \mathbb{L}_2(\mathcal{Z}(\mathbf{e}_3; \Theta))$, $\|\cdot\|_{\mathbb{L}_\infty} := \|\cdot\|_{\mathbb{L}_\infty(\mathcal{Z}(\mathbf{e}_3;\Theta))}$, denote by $\mathbf{A}_i$ the ith column of $\mathbf{A}$ and $\mathcal{I} := \{i : u_i^* \neq 0\}$.

Let $\mathcal{H}_t^d f = \sum_{i=1}^d u_i S_i$ and $\mathcal{H}_t f = \sum_{i=1}^{d_t} u_i S_i$, where $(u_1, \ldots, u_{d_t})^\top = \Lambda^{-1}\mathbf{A}^\top \bar{\mathbf{f}}$, $\bar{\mathbf{f}} := \bar{w}\mathbf{f}$. By Theorem 4.1(ii), we have

$$\|\mathcal{H}_t^d f - \mathcal{H}_t f\|_{\mathbb{L}_2}^2 = \frac{4\pi}{n\kappa_1}\sum_{i=1}^n (\mathcal{H}_t^d f(\mathbf{x}_i) - \mathcal{H}_t f(\mathbf{x}_i))^2 \leq \frac{4\pi}{\kappa_1}\|f\|_{\mathbb{L}_\infty}^2. \tag{4.3}$$

By Theorem 4.3(ii), $u_i^* = \lambda_i^{-1}(\mathbf{A}^\top \mathbf{b})_i$, $\forall i \in \mathcal{I}$ and $u_i^* = 0$, $\forall i \notin \mathcal{I}$. Then, we have

$$\|\mathcal{H}_t^* f - \mathcal{H}_t^d f\|_{\mathbb{L}_2}^2 = \sum_{i=1}^d \lambda_i |u_i^* - u_i|^2 = \sum_{i \in \mathcal{I}} \lambda_i |u_i^* - u_i|^2 + \sum_{i \notin \mathcal{I}} \lambda_i |u_i|^2$$

$$\leq \sum_{i\in\mathcal{I}} \frac{|\mathbf{A}_i^\top(\mathbf{b}-\bar{\mathbf{f}})|^2}{\lambda_i} + \frac{4\pi}{\kappa_1}\|f\|_{\mathbb{L}_\infty}^2 = \sum_{i\in\mathcal{I}} \frac{|\bar{w}\mathbf{A}_i^\top\boldsymbol{\epsilon}|^2}{\lambda_i} + \frac{4\pi}{\kappa_1}\|f\|_{\mathbb{L}_\infty}^2$$

$$\leq \bar{w}^2\|\boldsymbol{\epsilon}\|^2 \sum_{i\in\mathcal{I}} \frac{\|\mathbf{A}_i\|^2}{\lambda_i} + \frac{4\pi}{\kappa_1}\|f\|_{\mathbb{L}_\infty}^2 = \frac{4\pi|\mathcal{I}|}{n\kappa_1}\|\boldsymbol{\epsilon}\|^2 + \frac{4\pi}{\kappa_1}\|f\|_{\mathbb{L}_\infty}^2, \tag{4.4}$$

where the first equality follows from Parseval's theorem, the first inequality follows from Theorem 4.1(ii), and the last equality follows from $\mathbf{A}^\top\mathbf{A} = \Lambda$. Thus,

$$\|\mathcal{H}_t^* f - \mathcal{H}_t f\|_{\mathbb{L}_2}^2 \leq \|\mathcal{H}_t^* f - \mathcal{H}_t^d f\|_{\mathbb{L}_2}^2 + \|\mathcal{H}_t^d f - \mathcal{H}_t f\|_{\mathbb{L}_2}^2 \leq \frac{4\pi|\mathcal{I}|}{n\kappa_1}\|\boldsymbol{\epsilon}\|^2 + \frac{8\pi}{\kappa_1}\|f\|_{\mathbb{L}_\infty}^2. \tag{4.5}$$

Then we obtain

$$\begin{aligned}\|\mathcal{H}_t^* f - f\|_{\mathbb{L}_2} =& \|\mathcal{H}_t^* f - \mathcal{H}_t f + \mathcal{H}_t f - f\|_{\mathbb{L}_2} \leq \|\mathcal{H}_t^* f - \mathcal{H}_t f\|_{\mathbb{L}_2} + \|\mathcal{H}_t f - f\|_{\mathbb{L}_2} \\ \leq& \sqrt{\frac{4\pi|\mathcal{I}|}{n\kappa_1}}\|\boldsymbol{\epsilon}\| + \sqrt{\frac{8\pi}{\kappa_1}}\|f\|_{\mathbb{L}_\infty} + \sqrt{\frac{16\pi}{\kappa_1}}E_t(f),\end{aligned}$$

where the second inequality follows from Theorem 4.1(iii). The proof is completed. □

Remark 4.5. (Remark on Theorem 4.4) From the proof of Theorem 4.4, we observe that: (i) if $d = d_t$, then (4.3) vanishes; (ii) if $u_i = 0$ for $i \notin \mathcal{I}$, then the last term in (4.4) vanishes; (iii) if (i) and (ii) hold simultaneously, the second term in both (4.5) and (4.2) vanishes.

5. Numerical experiments. In this section, we present numerical experiments for numerical integration, hyperinterpolation and sparse approximation on spherical zones. We denote by $\mathcal{X}_n := \{\mathbf{x}_1, \ldots, \mathbf{x}_n\}$ the spherical zone t-designs on a spherical zone $\mathcal{Z}(\mathbf{z}; \Theta)$, $(x)_+ = \max\{x, 0\}$, $\forall x \in \mathbb{R}$, $\mathbf{e}_1 = (1, 0, 0)^\top$ and $\mathbf{e}_2 = (0, 1, 0)^\top$.

5.1. Numerical integration. Let $\mathbf{x} = (x, y, z)^\top \in \mathbb{S}^2$, we consider the following functions for numerical integration and hyperinterpolation,

$$\begin{aligned} f_1(\mathbf{x}) &= ((1/4 - (x - 1/\sqrt{18})^2 + (y - 1/\sqrt{18})^2 + (z - 4/\sqrt{18})^2)_+)^3, \\ f_2(\mathbf{x}) &= \exp(x + y + z) + 150(y - \cos(\pi/3))_+^3, \\ f_3(\mathbf{x}) &= \cos(10(x + y + z)), \end{aligned}$$

where f_1 has support on a spherical cap $\mathcal{C}(\bar{\mathbf{x}}; \arccos(7/8))$ with $\bar{\mathbf{x}} = (1, 1, 4)^\top/\sqrt{18}$ and is nonsmooth at the boundary of its support; f_2 is a function over the sphere and nonsmooth at the boundary of the spherical cap $\mathcal{C}(\mathbf{e}_2; \pi/3)$, and f_3 is a smooth function on the sphere.

We choose the spherical zones

$$\Gamma_1 := \mathcal{Z}(\bar{\mathbf{x}}; \Theta_1) \quad \text{and} \quad \Gamma_2 = \Gamma_3 := \mathcal{Z}(\mathbf{e}_3; \bar{\Theta}),$$

where $\Theta_1 = (\pi/25, \arccos(7/8))^\top$ and $\bar{\Theta} = (\pi/3, \pi/2)^\top$. The 3D view of f_i on $\Gamma_i, i = 1, 2, 3$ are shown in Fig.3 and Fig.4.

The approximate values of $\mathcal{I}_{\Gamma_i}(f_i) := \int_{\Gamma_i} f_i(\mathbf{x}) d\omega(\mathbf{x})$, $i = 1, 2, 3$ computed by using Matlab command "integral2" are $\mathcal{I}_{\Gamma_1}(f_1) := 0.0023640$, $\mathcal{I}_{\Gamma_2}(f_2) := 12.7842907$, and $\mathcal{I}_{\Gamma_3}(f_3) := -0.1589865$.

We show the absolute errors $|\mathcal{I}_{\Gamma_i}(f_i) - \frac{4\pi}{n\kappa_1}\sum_{j=1}^n f_i(\mathbf{x}_j)|$, $\mathbf{x}_j \in \mathcal{X}_n$, $i = 1, 2, 3$ as a function of degree t in Fig.3 and Fig.4.

For f_1, which is a zonal function, the sets $\mathcal{X}_n$ are induced by spherical t-designs with $(t+1)^2$ points [31], that is constructed following Theorem 3.6.

For f_2 and f_3, the spherical zone t-designs $\mathcal{X}_n$ are constructed by (3.9), where we use spherical t-designs with $(t+1)^2$ points [31] and $\zeta_j = 2\pi j/(t+1)^3$, $j = 1, \ldots, (t+1)^2$. We also compare the results with that of choosing $\zeta_j = 0$, $j = 1, \ldots, (t+1)^2$. See Fig.4 (b) and (e) .

In addition, for f_2 and f_3, we compare the results of using spherical zone t-designs $\mathcal{X}_n$ and $\mathcal{X}_{n'}^{\mathcal{Y}}$ which are induced from spherical t-designs only (see (3.7)), see Fig.4 (c) and (d). The spherical zone t-designs $\mathcal{X}_n$ in Fig.4 (c) and (d) are constructed using spherical t-designs with $N = t^2/2 + t + O(1)$ points [31] and $\zeta_j = 2\pi j/((t+1)N)$, $j = 1, \ldots, N$. The sets $\mathcal{X}_{n'}^{\mathcal{Y}}$ are induced from spherical t'-designs with $n' = (t'+1)^2$ points. The x-coordinates at the top and bottom in both Fig.4 (c) and (d) are degrees t' and t, respectively, such that $n' \geq n$.

From Fig.4, we see that spherical zone t-designs are efficient for numerical integration on spherical zones for smooth and nonsmooth functions. Moreover, spherical zone t-designs constructed using n distinct ζ_j perform better than using the same ζ_j, achieve smaller absolute errors and are more stable for different functions.

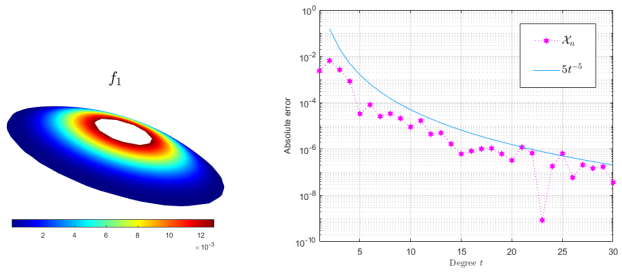

FIG. 3. *Left: 3D view of* f_1 *on* Γ_1 *; Right: absolute errors* $|\mathcal{I}_{\Gamma_1}(f_1) - \frac{4\pi}{n\kappa_1}\sum_{j=1}^{n} f_1(\mathbf{x}_j)|$.

5.2. Hyperinterpolation approximation. We show the hyperinterpolation approximation of f_1 on $\mathcal{Z}(\bar{\mathbf{x}}; \Theta_1)$, f_2 and f_3 on Γ_2 and Γ_3, respectively. We choose $\mathcal{X}_n$ to be a spherical zone 60-design with $n = 226,981$ constructed based on a spherical 60-design with 3721 points and $\zeta_j = 2\pi j/n$, $j = 1, \ldots, n$ to estimate the approximation errors. The $\mathbb{L}_2$ norm of the approximation error is estimated by

$$\|\mathcal{H}_t f_i - f_i\|_{\mathbb{L}_2(\Gamma_i)} \approx \left(\sum_{j=1}^{n} \frac{4\pi}{n\kappa_1} |f_i(\mathbf{x}_j) - \mathcal{H}_t f_i(\mathbf{x}_j)|^2\right)^{\frac{1}{2}}, \quad \mathbf{x}_j \in \mathcal{X}_n. \tag{5.1}$$

For each t, we estimate the uniform error by

$$\|\mathcal{H}_t f_i(\mathbf{x}) - f_i(\mathbf{x})\|_{\mathbb{L}_\infty(\Gamma_i)} \approx \max_{\mathbf{x}\in\mathcal{X}^\circ} |f_i(\mathbf{x}) - \mathcal{H}_t f_i(\mathbf{x})|, \tag{5.2}$$

where $\mathcal{X}^\circ \subset \Gamma_2$ is a set of generalized spiral points [7] with 250,000 points. The results are shown in Figure 5. We observe that spherical zone designs and Slepian functions are efficient for hyperinterpolation approximation on spherical zones. We choose $t = 30$ to show the pointwise errors. For f_1, the pointwise errors are significantly smaller for $t \geq 3$. For f_2 the largest pointwise error occurs at the boundary of the spherical cap $\mathcal{C}(\mathbf{e}_2; \pi/3)$ where it is nonsmooth. And for f_3, the largest pointwise error occurs at the boundary of $\mathcal{Z}(\mathbf{e}_3; \bar{\Theta})$.

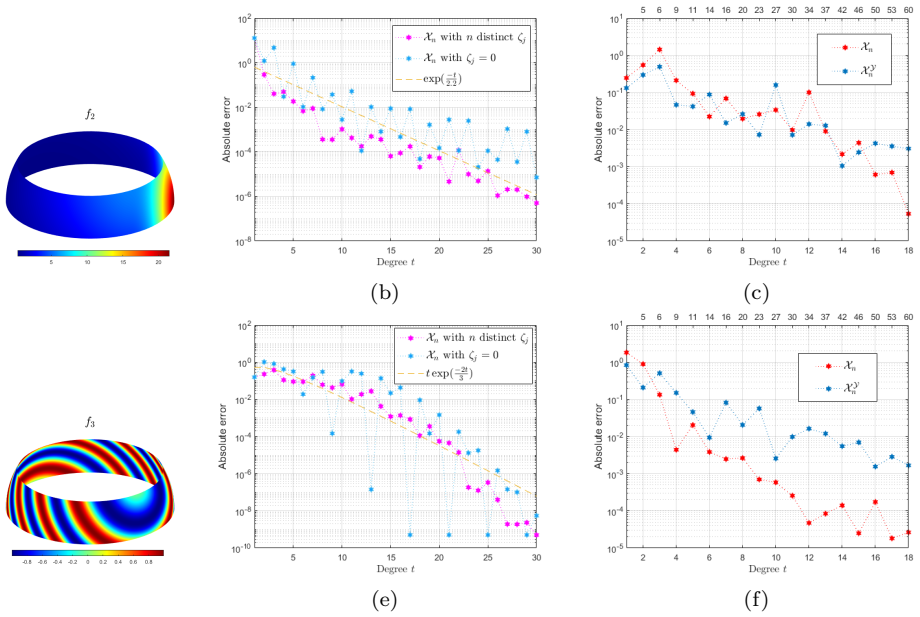

FIG. 4. *(b) and (c) are the absolute errors of f_2; (e) and (f) are the absolute errors of f_3.*

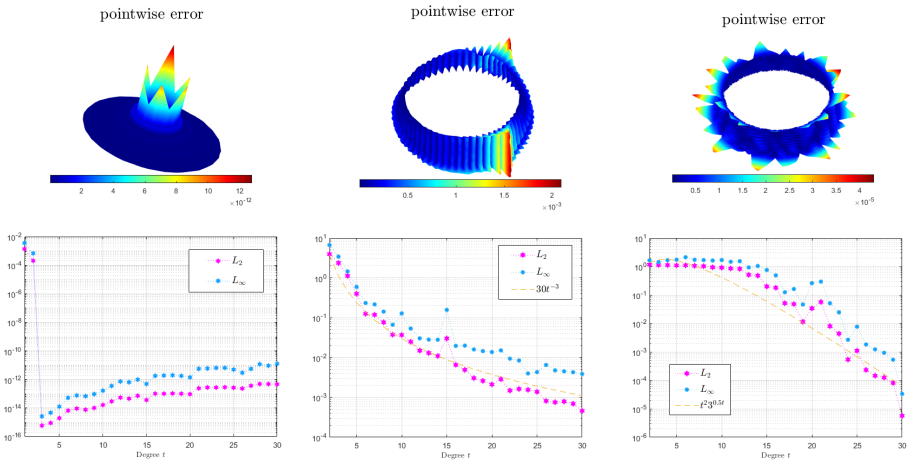

FIG. 5. *Hyperinterpolation approximation errors and pointwise errors of f_1 (left column), f_2 (middle column) and f_3 (right column) for $t = 30$.*

5.3. Sparse approximation. We choose the following test function

$$f_4(\mathbf{x}) = \sum_{j=1}^{6} h(\|\mathbf{x} - \mathbf{x}_j\|), \quad \forall \mathbf{x} \in \mathbb{S}^2,$$

where $h(x) = (1-x)_+^8(32x^3+25x^2+8x+1)$, $\forall x \in \mathbb{R}$ is the Wendland function [13], $\mathbf{x}_1 = \mathbf{e}_1$, $\mathbf{x}_2 = (1/2, \sqrt{3}/2, 0)^\top$, $\mathbf{x}_3 = (-1/2, \sqrt{3}/2, 0)^\top$, $\mathbf{x}_4 = -\mathbf{e}_1$, $\mathbf{x}_5 = (-1/2, -\sqrt{3}/2, 0)^\top$ and $\mathbf{x}_6 = (1/2, -\sqrt{3}/2, 0)^\top$.

We choose the spherical zone $\mathcal{Z}(\mathbf{e}_3; \tilde{\Theta})$ with $\tilde{\Theta} = (\pi/3, 2\pi/3)^\top$. And $d := S_h =$

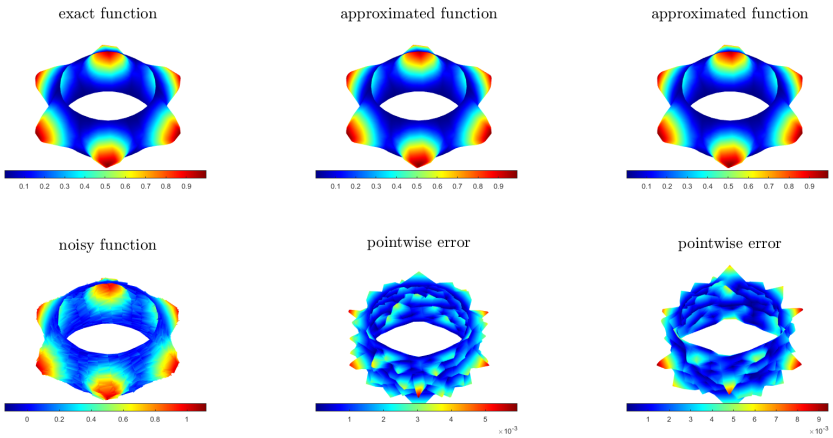

FIG. 6. *Sparse approximation results of f_4 on $\mathcal{Z}(\mathbf{e}_3;\tilde{\Theta})$ with $\sigma = 0.05$, where the second and third columns are the results solved by problem (4.1) and problem (5.3), respectively.*

128. We see from Figure 7 that f_4 is highly located in the spherical zone. Then, we choose $t = 15$ and $\mathcal{X}_n$ to be a spherical zone 31-design with $n = 15438$ on the spherical zone constructed from a symmetric spherical 31-design with 498 points [31] and $\zeta_j = 2\pi j/n$, $j = 1, \ldots, n$.

We also show the approximation results solved by the l_1 norm regularized optimization problem (see for example [3]), that is,

$$\min_{\mathbf{u}\in\mathbb{R}^d} \frac{1}{2}\|\mathbf{A}\mathbf{u} - \mathbf{b}\|^2 + \mu\|\mathbf{u}\|_1. \tag{5.3}$$

For problem (4.1), we set $\mu = 0.02$ and $\delta = \mu/\|\mathbf{A}^\top\mathbf{b}\|_1$. For problem (5.3), we set $\mu = 0.001$ if $\sigma = 0.05$, $\mu = 0.0032$ if $\sigma = 0.1$. We test ten times and report the average values.

We show the approximation results in Table 1, where we also show the results solved by problem (5.3) with $\mu = 0.02$, $\bar{\mathbf{u}}$ denotes the local minimizer, "nnz($\bar{\mathbf{u}}$)" denotes the number of nonzero elements in $\bar{\mathbf{u}}$, $\mathbb{L}_2 := \mathbb{L}_2(\mathcal{Z}(\mathbf{e}_3;\tilde{\Theta}))$, $\mathbb{L}_\infty := \mathbb{L}_\infty(\mathcal{Z}(\mathbf{e}_3;\tilde{\Theta}))$ are estimated following (5.1) and (5.2), respectively.

We see from Table 1 that the capped-l_1 regularized problem (4.1) performs better. We show the pointwise errors solved by problems (4.1) and (5.3) in Figures 6 and 7. We observe that the largest error occurs at the boundary or the nonsmooth point of the function.

TABLE 1
Sparse approximation results of f_4 on $\mathcal{Z}(\mathbf{e}_3;\tilde{\Theta})$ solved by problem (4.1) and problem (5.3).

	$\sigma = 0.05$			$\sigma = 0.1$		
Problem	nnz($\bar{\mathbf{u}}$)	$\mathbb{L}_2$	$\mathbb{L}_\infty$	nnz($\bar{\mathbf{u}}$)	$\mathbb{L}_2$	$\mathbb{L}_\infty$
capped-l_1	8	0.0044	0.0057	8	0.0066	0.0088
l_1	42.9	0.0064	0.0099	20.2	0.017	0.0165
l_1 ($\mu = 0.02$)	6.8	0.0556	0.0544	6.6	0.0553	0.0558

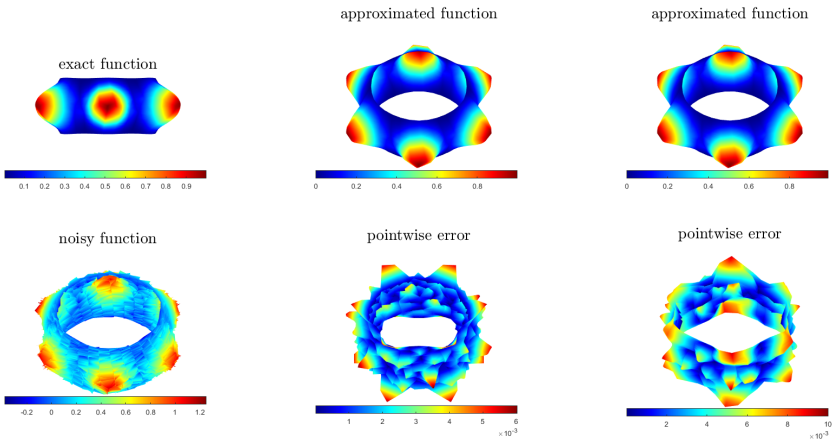

FIG. 7. *Sparse approximation results of f_4 on $\mathcal{Z}(\mathbf{e}_3;\tilde{\Theta})$ with $\sigma = 0.1$, where the second and third columns are the results solved by problem (4.1) and problem (5.3), respectively.*

6. Conclusion. In this paper, we propose spherical zone t-designs, which provide equal weight quadrature rules with polynomial exactness t on a spherical zone $\mathcal{Z}(\mathbf{z};\Theta)$ with center $\mathbf{z} \in \mathbb{S}^2$ and angular radius $\Theta = (\underline{\theta}, \bar{\theta})^\top$ satisfying $0 \le \underline{\theta} < \bar{\theta} \le \pi$. The spherical zone t-design is constructed based on spherical t-designs and trapezoidal rules on $[0, 2\pi]$ with polynomial exactness t. We compare various spherical zone t-designs constructed from a spherical t-design and different sets of quadrature nodes of the trapezoidal rule on $[0, 2\pi]$ with polynomial exactness t. We show that using spherical t-designs only we can obtain quadrature rules with equal weight and polynomial exactness t for spherical zonal polynomials on spherical zones. Moreover, we apply the spherical zone t-designs and Slepian functions to numerical integration, hyperinterpolation, and sparse approximation on spherical zones and derive error bounds of the approximations. Numerical experiments show that spherical zone t-designs constructed with different $\{\zeta_j\}$ have better performance than using the same $\{\zeta_j\}$ and are promising for approximation on spherical zones.

Note that, in [1, 11], the authors proposed methods for computing spherical t-designs with $O(t^2)$ points. However, these methods cannot be directly adapted to spherical zones, since Proposition 2.1 in [1] does not hold over spherical zones. The construction of spherical zone t-designs with $O(t^2)$ points remains an open problem and warrants our further study.

Acknowledgement. We would like to thank Prof. Ian Sloan for detailed discussions on this paper during his visit in The Hong Kong Polytechnic University. We also thank the associate editor and two referees for their very helpful comments.

REFERENCES

[1] C. An, X. Chen, I. H. Sloan, and R. S. Womersley, *Well conditioned spherical designs for integration and interpolation on the two-sphere*, SIAM J. Numer. Anal., 48 (2010), pp. 2135–2157.
[2] C. An, X. Chen, I. H. Sloan, and R. S. Womersley, *Regularized least squares approximations on the sphere using spherical designs*, SIAM J. Numer. Anal., 50 (2012), pp. 1513–1534.
[3] C. An and H.-N. Wu, *Lasso hyperinterpolation over general regions*, SIAM J. Sci. Comput.,

43 (2021), pp. A3967–A3991.
[4] K. Atkinson, *An Introduction to Numerical Analysis*, John Wiley & Sons, 1991.
[5] K. Atkinson and W. Han, *Spherical Harmonics and Approximations on the Unit Sphere: An Introduction*, Springer Science & Business Media, 2012.
[6] E. Bannai and E. Bannai, *A survey on spherical designs and algebraic combinatorics on spheres*, Eur. J. Combin., 30 (2009), pp. 1392–1425.
[7] R. Bauer, *Distribution of points on a sphere with application to star catalogs*, J. Guid. Control Dynam., 23 (2000), pp. 130–137.
[8] S. Bernstein, *On quadrature formulas with positive coefficients*, Izv. Akad. Nauk SSSR Ser. Mat, 4 (1937), pp. 479–503.
[9] W. Bian and X. Chen, *A smoothing proximal gradient algorithm for nonsmooth convex regression with cardinality penalty*, SIAM J. Numer. Anal., 58 (2020), pp. 858–883.
[10] A. Bondarenko, D. Radchenko, and M. Viazovska, *Optimal asymptotic bounds for spherical designs*, Ann. Math., (2013), pp. 443–452.
[11] X. Chen, A. Frommer, and B. Lang, *Computational existence proofs for spherical t-designs*, Numer. Math., 117 (2011), pp. 289–305.
[12] X. Chen and R. S. Womersley, *Spherical designs and nonconvex minimization for recovery of sparse signals on the sphere*, SIAM J. Imaging Sci., 11 (2018), pp. 1390–1415.
[13] A. Chernih, I. H. Sloan, and R. S. Womersley, *Wendland functions with increasing smoothness converge to a Gaussian*, Adv. Computat. Math., 40 (2014), pp. 185–200.
[14] F. Dai and H. Wang, *Positive cubature formulas and Marcinkiewicz–Zygmund inequalities on spherical caps*, Constr. Approx., 31 (2010), pp. 1–36.
[15] P. Delsarte, J.-M. Goethals, and J. J. Seidel, *Spherical codes and designs*, in Geom. Dedicata, Elsevier, 1991, pp. 68–93.
[16] P. Gautron, J. Kivánek, S. N. Pattanaik, and K. Bouatouch, *A novel hemispherical basis for accurate and efficient rendering*, in Proc. EGSR 15th Euro-Graph. Conf. Rendering Techn., (2004), pp. 321–330.
[17] Z. He, S. Han, A. Gómez, Y. Cui, and J.-S. Pang, *Comparing solution paths of sparse quadratic minimization with a Stieltjes matrix*, Math. Program., 204 (2024), pp. 517–566.
[18] K. Hesse and R. S. Womersley, *Numerical integration with polynomial exactness over a spherical cap*, Adv. Comput. Math., 36 (2012), pp. 451–483.
[19] C. Li and X. Chen, *Spherical designs for approximation on spherical caps*, SIAM J. Numer. Anal., 62 (2024), pp. 2506–2528.
[20] S. B. Lin, D. Wang, and D. X. Zhou, *Sketching with spherical designs for noisy data fitting on spheres*, SIAM J. Sci. Comput., 46 (2024), pp. A313–A337.
[21] H. Mhaskar, *Local quadrature formulas on the sphere, II*, In: Neamtu, M., Saff, E.B. (eds.) Advances in Constructive Approximation, (2004), pp. 333–344.
[22] H. N. Mhaskar, *Local quadrature formulas on the sphere*, J. Complexity, 20 (2004), pp. 753–772.
[23] J. S. Pang, M. Razaviyayn, and A. Alvarado, *Computing B-stationary points of nonsmooth dc programs*, Mathematics of Operations Research, 42 (2017), pp. 95–118.
[24] P. D. Seymour and T. Zaslavsky, *Averaging sets: a generalization of mean values and spherical designs*, Adv. Math., 52 (1984), pp. 213–240.
[25] F. J. Simons, F. Dahlen, and M. A. Wieczorek, *Spatiospectral concentration on a sphere*, SIAM Rev., 48 (2006), pp. 504–536.
[26] I. H. Sloan, *Polynomial interpolation and hyperinterpolation over general regions*, J. Approx. Theory, 83 (1995), pp. 238–254.
[27] A. Sommariva and M. Vianello, *Near-algebraic Tchakaloff-like quadrature on spherical triangles*, Appl. Math. Lett., 120 (2021), p. 107282.
[28] A. Sommariva and M. Vianello, *Numerical hyperinterpolation over spherical triangles*, Math. Comput. Simulat., 190 (2021), pp. 15–22.
[29] L. N. Trefethen and J. Weideman, *The exponentially convergent trapezoidal rule*, SIAM Rev., 56 (2014), pp. 385–458.
[30] Y. G. Wang, Q. T. Le Gia, I. H. Sloan, and R. S. Womersley, *Fully discrete needlet approximation on the sphere*, Appl. Computat. Harmon. Anal., 43 (2017), pp. 292–316.
[31] R. S. Womersley, *Efficient spherical designs with good geometric properties*, http://web.maths.unsw.edu.au/ rsw/Sphere /EffSphDes/, (2015).